Life-cycle modelling of concrete cracking and reinforcement corrosion in concrete bridges: A case study

Shilun Chen[1], Colin Duffield[2], Saeed Miramini[3], Babar Nasim Khan Raja[4], Lihai Zhang[5,*]

[1] Ph.D. student, Department of Infrastructure Engineering, B404, Engineering Block B, University of Melbourne, Victoria 3010, Australia. shilunc@student.unimelb.edu.au

[2] Professor., Department of Infrastructure Engineering, D212, Engineering Block D, University of Melbourne, Victoria 3010, Australia. colinfd@unimelb.edu.au

[3] Dr.Eng./Lecturer, Department of Infrastructure Engineering, C501, Engineering Block C, University of Melbourne, Victoria 3010, Australia. s.miramini@unimelb.edu.au

[4] Ph.D. student, Department of Infrastructure Engineering, D402, Engineering Block D, University of Melbourne, Victoria 3010, Australia. babarr@student.unimelb.edu.au

[5,] *Associate Professor., Department of Infrastructure Engineering, D210, Engineering Block D, University of Melbourne, Victoria 3010, Australia. lihzhang@unimelb.edu.au (Corresponding author)

Abstract

The development of effective life cycle management strategies for transport infrastructure assets is of importance for meeting the defined public policies and levels of service. In the last decades, much progress has been made in assessing the life-cycle performance of bridges using reliability-based approaches. However, the goal of developing a comprehensive life-cycle performance assessment framework for bridges has not been fully achieved. This is due to the uncertainties surrounding model parameters as well as the correlation between these parameters (e.g. the complex correlation between the reinforcement corrosion and the concrete cracking). It becomes more challenging due to the limited access to bridge inspection data by bridge research communities resulting from confidentiality issues. Using a typical highway concrete bridge as a case study, the present study systematically investigated the impact of concrete crack induced reinforcement corrosion on the serviceability of concrete bridges by developing an engineering reliability-based approach involving an auto-regressive crack propagation model and a steel corrosion prediction model. The model parameters were calibrated using the eight-year inspection

data of an operating bridge. The influence of different external environments in the reinforcement corrosion, ultimately the residual life of the bridges, was also investigated through conducting a series of parametric studies. Based on the collected bridge inspection data, the model results predict that, although the surface crack of a RC bridge is repairable through periodic maintenance, the corrosion of the steel bars in the bridge still continues over time with a corrosion rate which depends on different maintenance intervention cycle periods (T_{cycle}). For example, reducing T_{cycle} from 12 years to 4 years could potentially prolong the service life of the bridge by around 15 years. The developed model could assist bridge managers to estimate the optimal T_{cycle} to prolong the service life of bridges.

Keywords

Reinforced concrete bridges; concrete cracks; steel corrosion; engineering reliability analysis; first-order second-moment (FOSM); auto-regressive model

1. Introduction

As one of the fundamental transport infrastructures, bridges continuously support social and economic development of the world. The consistently operational performance of bridges plays a critical role for both public and private sectors. Bridge inspection, maintenance and repair become daily routines for maintaining the health of bridges [1]. However, the service life of many bridges in the world is expected to be less than their design life due to the continuous deterioration of bridges induced by daily traffic loading and environmental conditions [2, 3]. Therefore, it becomes increasingly important to maintain and repair the deteriorated bridges in a timely and cost-effective manner.

Concrete is one of the commonly used construction materials for bridges. Concrete cracking is generally used as one of the primary indicators for assessing the severity of reinforced concrete (RC) bridge deterioration [4]. Cracks in RC bridges can be classified into two main types, *i.e.* loading cracks and non-loading cracks [5]. While the non-loading cracks are mainly caused by environmental factors (*e.g.* cyclic changes in temperature and moisture), the loading cracks are caused by external loading imposed on the bridges (*e.g.* traffic loading, earthquake, etc.) [6, 7]. The crack development in RC bridges over time could result in the corrosion of reinforcements in concrete, delamination, which affects the mechanical properties of concrete material, and ultimately reduce the service life of a bridge [8]. Most importantly, corrosion of steel bars in concrete induced by cracking may lead to the failure of the bridges. Concrete cracking and corrosion of reinforcing steel bars have a bilateral influence on each other [9]. During the corrosion process of steel bars, the hydrated ferric oxide (*i.e.* rust), which is a larger substance than the original ferrous hydroxide, causes the expansion of the internal space between concrete and reinforcing steel bars. This produces a higher inner pressure in concrete which results in the formation of cracks around the interface between concrete and steel bars [10]. As the corrosion proceeds, cracks can propagate from the inner surface to the external surface, *i.e.* so-called

corrosion-induced cracking. Although a high alkaline environment in concrete can hinder the corrosion of steel bars through the formation of a passive layer, cracks in concrete could provide a pathway for chloride ions, acidic ions, carbon dioxide and other substances to corrode the steel bars in concrete [11]. In addition, under sulfate attack, formation of ettringite could happen in concrete [12], ultimately lead to concrete cracking due to expansion of ettringite within the concrete [13]. Previous experimental studies have shown that the steel bar corrosion in concrete depends on crack characteristics [14], such as width, types and frequency, particularly at the initial stage of corrosion.

Several theoretical studies have been carried out to investigate the relationship between corrosion of steel bars and crack development in RC structure members [15-19]. Based on the relationship between residual load capacity, surface crack width and corrosion of steel bars of a RC structure, an empirical model is proposed to predict the structural performance of corroded RC structures [20]. In addition, a theoretical model for crack widths has been developed to assess the serviceability of the RC structures based on the concept of fracture energy under combined reinforcement corrosion and applied loading effects [21]. Further, a mathematical model was proposed to predict the service life of the RC bridge structures exposed to chloride environment based on Fick's second law [22]. Moreover, to account for the uncertainties of structural deterioration induced by the combined effects of progressive loading (corrosion and cracking) and extreme loading (earthquake and impact), a stochastic model was used to predict the time-dependent performance of infrastructures using structural reliability analysis with the aim of improving decision-making for maintenance and replacement of infrastructures [2]. Furthermore, because of the importance of failure probability assessment for structural systems which have different uncertain inputs [23], a probabilistic model regarding structural deterioration subject to corrosion was developed to predict the probability of failure (PoF) of reinforcing steels in a RC bridge deck in a marine environment throughout its 75 years' service life [24].

Although much research work has been done in last decades to develop the reliability-based life-cycle performance model for bridges [25-27], the accuracy of the realistic model forecasting of future bridge performance is much dependent on the accurate determination of the model parameters. This is rather challenging due to a range of uncertainties surrounding these parameters resulting from the limited measurement data as well as the correlation between these parameters, e.g. the corrosion rate of reinforcing steel bars is closely correlated to the crack propagation of concrete. Although autoregressive processes have been implemented to predict the long-term deterioration of concrete structures [28], the determination of the model coefficients depends on the collection of a large amount of historical data. In addition, even if several reliability-based mathematical model have been established to simulate the reinforcement corrosion of highway bridges [29], the chloride diffusion coefficient and corrosive rate of reinforcements are significantly affected by the crack propagation of concrete cover over time. Without historical crack measurement data, the long-term reinforcement corrosion behavior cannot be correctly modelled. Using the historical data collected from bridge inspection, the purpose of this study is to develop an engineering reliability analysis (ERA)-based framework to assess the life-cycle performance of RC bridges subject to reinforcement corrosion by concrete cracking. The current research represents the first step towards fundamental understanding of the concrete cracking induced reinforcement corrosion, which could potentially contribute to the development of effective bridge maintenance strategies.

2. Method

2.1 ERA-based framework for life-cycle condition assessment of bridges

Figure 1 shows the details of developed ERA-based framework for assessing the life-cycle performance of the RC bridges which are gradually deteriorating resulting from steel bar corrosion due to the development of concrete cracking. First, the initial crack characteristics (e.g. crack width) at time t_0 are quantified through data collection via bridge inspection. Then, the

development of crack characteristics over time is captured from next bridge inspection at time $t_0+\Delta t$ (Δt: bridge inspection time interval). Based on collected historical data, the long-term crack propagation is predicted using an auto-regressive (AR) approach (Equation (1)) [30, 31]. The accuracy of autoregression model prediction could be improved with the collection of more crack measurement data over time. Using chloride diffusion model and steel corrosion model (Equation (8)-(14)), the long-term corrosion behaviour of steel bars can be estimated based on the time-dependent crack characteristics (see Figure 2). Finally, the change reliability index (β) of the bridge structures can be predicted based on the codes of practice requirements of bridge design and construction (*e.g.* maximum allowable crack width, W_0).

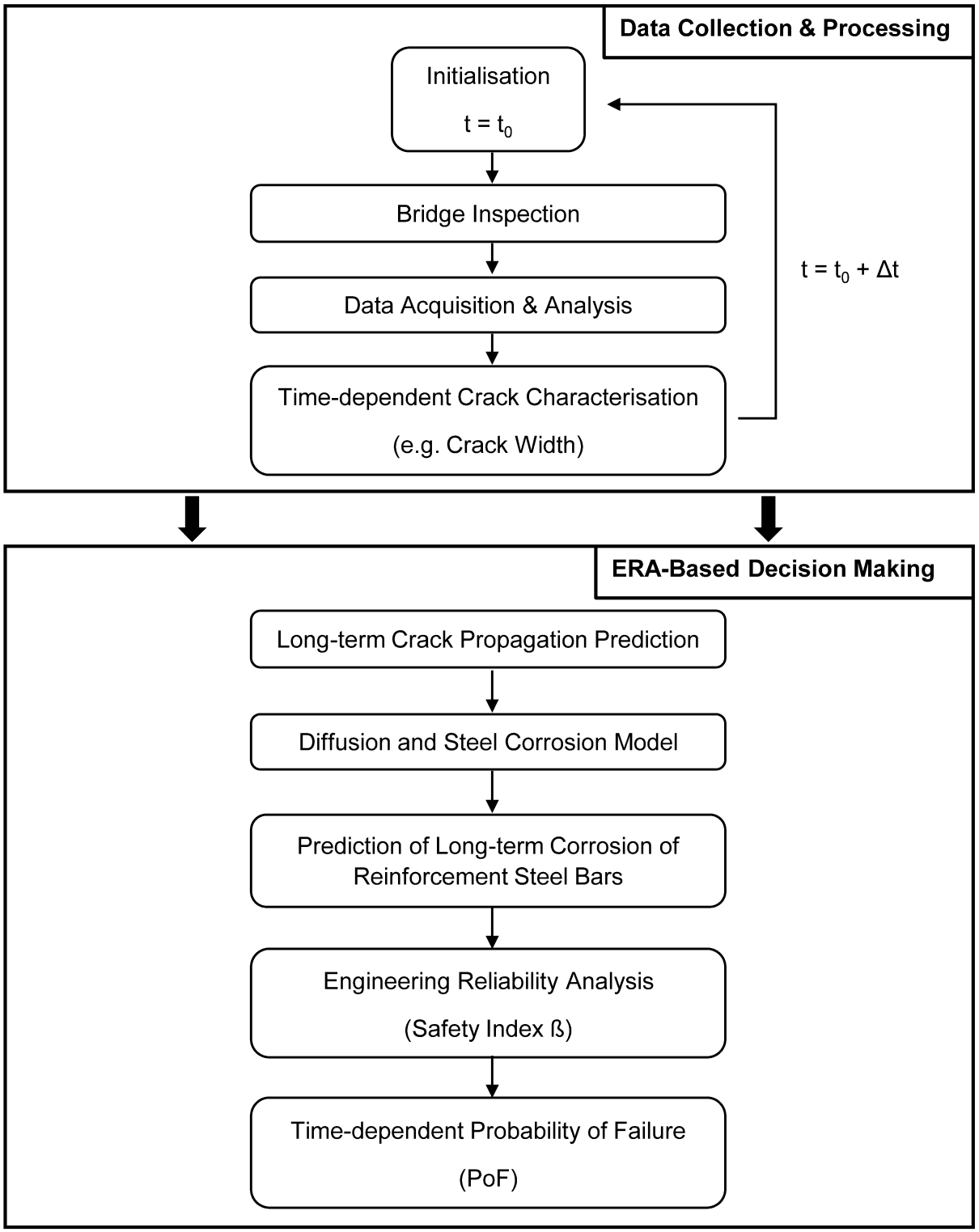

127

128 Figure 1 – Proposed framework for life-cycle condition assessment of reinforced concrete
129 structures using engineering reliability analysis. ERA, engineering reliability analysis.

As shown in Figure 2, the developed framework could be implemented to assess the PoF of a bridge under different maintenance intervention cycle periods (T_{cycle}). It shows the time-dependent crack propagation under different routine bridge inspection intervals (Δt). When crack width W_t approaches W_0, maintenance intervention is required for crack treatment under a certain T_{cycle}. As shown in Equations (12) - (14), it is assumed that the rate of the reinforcement corrosion depends on the crack width. Initially (e.g. short time after maintenance, $t < T_1$), the rate of corrosion is relatively low when the concrete crack width is relatively small ($W_t < W_1$). Over time, the rate of corrosion accelerates when the crack width is over a certain threshold (i.e. W_0). The details are described in Figure 2.

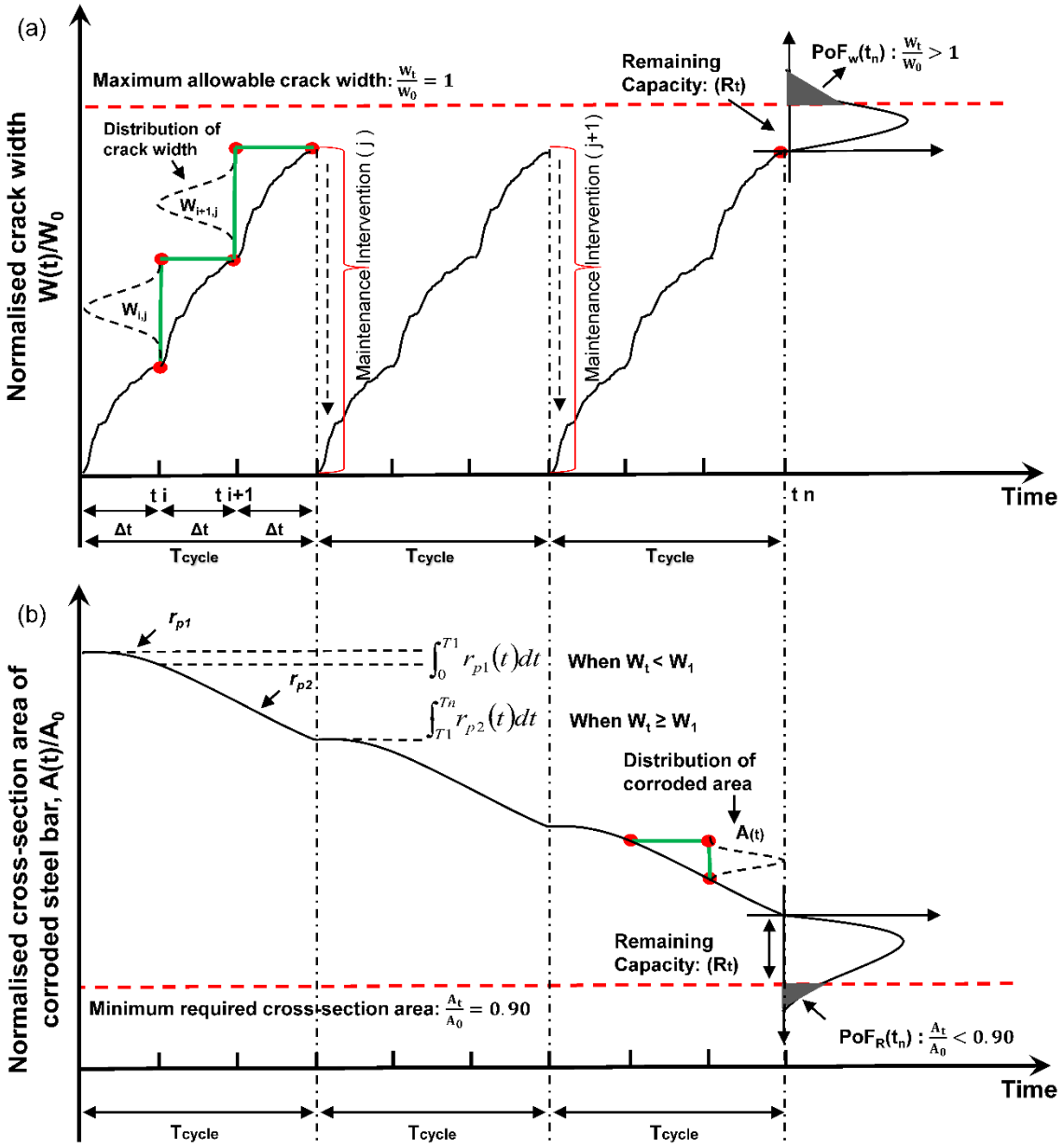

139

140 Figure 2 – (a) An engineering reliability analysis (ERA)-based approach for assessing crack
141 propagation under maintenance intervention cycle period T_{cycle} (W_0: maximum allowable crack
142 width, W_1: crack width inducing higher diffusion coefficient and corrosion rate, Δt: inspection time
143 interval and T_{cycle}: maintenance intervention cycle period); (b) an ERA-based approach for
144 assessing reinforcement steel corrosion in concrete under crack maintenance intervention cycle

period T_{cycle} (r_{p1}: steel corrosion rate when $W_t < W_1$, r_{p2}: steel corrosion rate when $W_t \geq W_1$ & A_0: initial cross-section area of steel bar).

2.2 Auto-regressive model for crack propagation prediction

While recent advance in artificial intelligence provide an innovative way to model crack in concrete bridges [32], a large amount of training data and the selection of the optimal algorithm are required. Considering the limited amount of inspection data available in this study, the autoregressive model was implanted to predict the long-term crack propagation due to its capability of modelling time-varying random process based on historical data [33]. The AR model has the capability of univariately forecasting time-series models which demonstrate the relationship between a single variable and its corresponding past values [34]. As a first step, by assuming that there is little change in environmental and loading conditions in recent years, the long-term prediction of crack width in concrete can be defined as a stationary process. That is,

$$W_t = \beta_1 W_{t-1} + \beta_2 W_{t-2} + \cdots + \beta_p W_{t-p} + \varepsilon_t \quad (1)$$

where P, as the order of auto-regressive process (AR(p)), represents the number of past values which will be included. P is defined by the highest time-lag order coefficient which is less than 0.05. At a given time t, ε_t is the random distribution of uncorrelated error with zero mean and variance, *i.e.* $\{\varepsilon_t\} \sim (0, \sigma^2)$. β is the AR coefficient with $|\beta| < 1$ [31, 35].

Hence, the predicted concrete crack width at time *t* can be expressed as,

$$W_t = \sum_{i=0}^{p} \beta_i W_{t-i} + \varepsilon_t \quad (2)$$

By applying the backward shift operator $\pi(B)$,

$$\pi(B) = \sum_{i=0}^{p} \beta_i B_i \quad (3)$$

Equation (2) can be written as,

$$W_t = \pi(B)W_{t-i} + \varepsilon_t \quad (4)$$

With consideration of periodic crack maintenance intervention, we obtain,

$$W_{t_{i,j}} = \begin{cases} \sum_{i=0,j=0}^{p} \beta_{i,j} W_{t-i,j} + \varepsilon_t & t_j < t < t_{j+1} \\ 0 & t = t_j \end{cases} \quad (5)$$

where j represents the j-th number of crack maintenance intervention after the i-th year of crack inspection. Using the indicator function $\mathbf{1}_{t_j}$ as shown below,

$$\mathbf{1}_{t_j} = \begin{cases} 1 & t_j < t < t_{j+1} \\ 0 & t = t_j \end{cases} \quad (6)$$

The crack width with time under different maintenance interventions can be expressed as,

$$W_{t_{i,j}} = \sum_{i=0,j=0}^{p} (\beta_{i,j} W_{t-i,j} + \varepsilon_t) * \mathbf{1}_{t_j} \quad (7)$$

2.3 Predicting corrosion of reinforcement steel bars in concrete

As shown in Figure 3, throughout the service life, the corrosion process of RC structures can be divided to the following two stages:

- Initial stage ($0<t<t_1$): At this stage, chloride ions gradually diffuse into concrete from external environment until the concentration of chloride ions on the surface of steel bars in concrete reaches to the maximum allowable threshold value ($C_{threshold}$) defined in design guidelines [11]. The thickness of concrete cover, concentration of chloride ions on concrete surface and diffusion coefficient of chloride ions play an important role in corrosion resistance at this stage.

- Propagation stage ($t>t_1$): At this stage, significant chloride ions induced corrosion of steel bars occurs and could cause the local damage of the RC structures [36, 37].

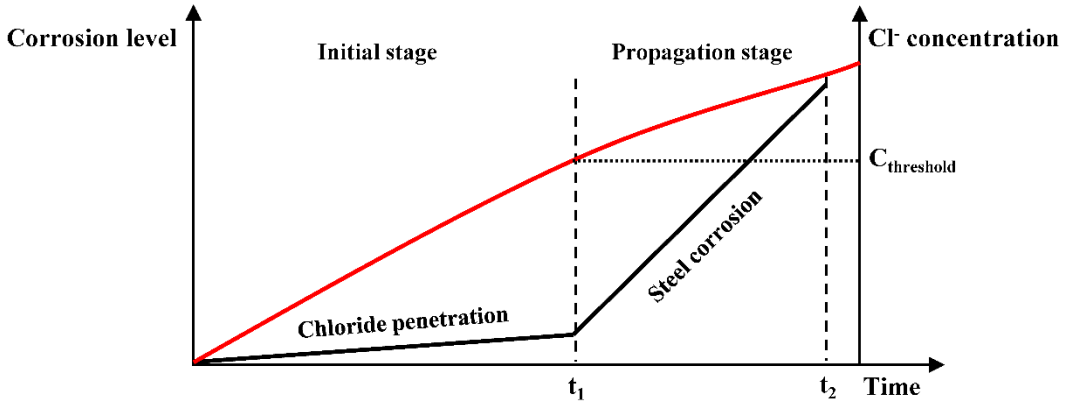

Figure 3 – Corrosion process of reinforcement steel bars in concrete [36, 37]

Initial stage:

The transport of mass through diffusive means is generally modelled using the Fick's second law [38, 39]. That is,

$$C(x,t) = kt\{\left(1+\frac{x^2}{Dt}\right)\operatorname{erf}\left(\frac{x}{2\sqrt{Dt}}\right) - \left(\frac{x}{\sqrt{\pi Dt}}\right)e^{\frac{-x^2}{4Dt}}\} \quad (8)$$

In this study, $C(x,t)$ is chloride concentration at depth x (mm) of concrete cover at time t (year). D is the diffusion coefficient (mm^2/year) which is much dependent on the porosity of the concrete and the volume fraction of aggregate in concrete [11, 12].

Propagation stage:

At this stage, the significant corrosion process of steel bars in concrete is triggered as the chloride concentration reaches to the threshold value ($C_{threshold}$ = 0.68% [11, 40-42]). In this study, the mass loss of steel bars in concrete was modelled using mathematical approach of Du et al. (2005) [9], which divides the corrosion of steel bars in concrete into two stages, i.e. (1) chemical reaction stage, and (2) the stage involving current flow with anode and cathode on surface of reinforcement

steel bars, leading to the transformation of iron into rust which sticks onto the surface of steel bars [43]. The rate of mass loss of steel bar (Q_{corr}) can be defined as,

$$Q_{corr} = \frac{M_0 - M_1}{M_0} \tag{9}$$

where M_0 is the initial weight of steel bar before corrosion started and M_1 is the weight of corroded steel bar. Using the empirical corrosion model proposed by [9], Equation (8) can be modified as,

$$Q_{corr} = 0.046 * \frac{r_{corr}}{d} * t \tag{10}$$

where r_{corr} is the corrosion rate of steel bar in a RC structure under certain environmental conditions ($\mu A/cm^2$), d is the diameter of non-corroded steel bar (mm). Thus, the time-dependent cross-section area of the corroded steel bars in concrete structure can be expressed as [9],

$$A_{t_{i,j}} = A_0(1 - Q_{corr}) \tag{11}$$

where A_0 is the initial cross-section area of non-corroded steel bar.

Previous studies have demonstrated that there is a positive correlation between the corrosion rate of bars in concrete and the surface crack width as shown in Figure 2 [9]. Let $\mathbf{1}_{(W_t)}$ be an indicator function for corrosion rate of steel bar under different crack widths on a concrete surface. It is assumed that the corrosion rate of a steel bar is r_1 when crack width W_t is less than W_1, while the corrosion rate of a steel bar is r_2 when W_t is greater than W_1. The indicator function $\mathbf{1}_{(W_t)}$ can be written as,

$$\mathbf{1}_{W_t,1} = \begin{cases} 1 & 0 < W_{t_{i,j}} < W_1 \\ 0 & W_{t_{i,j}} \geq W_1 \end{cases} \tag{12}$$

$$\mathbf{1}_{W_t,2} = \begin{cases} 0 & 0 < W_{t_{i,j}} < W_1 \\ 1 & W_{t_{i,j}} \geq W_1 \end{cases} \tag{13}$$

Combining Equations (10) and (12), the time-dependent cross-section area of the corroded steel bars in concrete structure due to the development of crack width can be expressed as,

$$A_{t_{i,j}} = A_0 * \left\{1 - \int_0^{\infty} \left[(0.046 * \frac{r_1}{d} * \mathbf{1}_{W_{t,1}}) + (0.046 * \frac{r_2}{d} * \mathbf{1}_{W_{t,2}})\right] dt\right\} \quad (14)$$

2.4 Life-cycle performance assessment of the bridges using ERA

The time dependent PoF of the bridges due to steel bar corrosion can be predicted using ERA. β can be calculated using first-order second-moment (FOSM) [44] with consideration of the first two moments which are mean and standard deviation of the random variables. In FOSM, the non-linear performance function is required to be linearised [45-47]. Considering $(X_1, X_2, \dots, X_n)$ as random variables, the non-linear function Z can be expressed as,

$$Z = f(X) = f(X_1, X_2, \dots, X_n) \quad (15)$$

Taylor series expansion with second-order terms leads to,

$$Z = f(\mu_X) + \sum_{i=1}^{n} \frac{\partial f}{\partial X_i} + \frac{1}{2} \sum_{i=1}^{n} \sum_{j=1}^{n} \frac{\partial f^2}{\partial X_i \partial X_j} (X_i - \mu_{X_i})(X_j - \mu_{X_j}) + \cdots \quad (16)$$

where μ_X are mean of these random variables $(\mu_{X_1}, \mu_{X_2}, \dots, \mu_{X_n})$. The second-order approximated mean of Z, *i.e.* $E(Z)$ can be obtained,

$$E(Z) = f(\mu_{X_1}, \mu_{X_2}, \dots, \mu_{X_n}) + \frac{1}{2} \sum_{i=1}^{n} \sum_{j=1}^{n} \frac{\partial f^2}{\partial X_i \partial X_j} Cov(X_i, X_j) \quad (17)$$

where $Cov(X_i, X_j)$ is the covariance of X_i and X_j.

$$Cov(X_i, X_j) = \rho_{X_i, X_j} * \sigma_{X_i} * \sigma_{X_j} \quad (18)$$

where σ_X is the standard deviation of these random variables $(\sigma_{X_1}, \sigma_{X_2}, \dots, \sigma_{X_n})$, ρ_{X_i, X_j} is coefficient of correlation between X_i and X_j.

In the FOSM analysis, the function Z is expanded by Taylor series expansion with first-order terms. That is,

$$Z = f(X_1, X_2, \dots, X_n) + \sum_{i=1}^{n} \frac{\partial f}{\partial X_i}\left(X_i - \mu_{X_i}\right) + \cdots \quad (19)$$

By applying the first-order approximation, $E(Z)$ can be defined as,

$$E(Z) \approx f\left(\mu_{X_1}, \mu_{X_2}, \dots, \mu_{X_n}\right) \quad (20)$$

The variance of function $Var(Z)$ with second-order approximation is,

$$Var(Z) \approx \sum_{i=1}^{n}\left(\frac{\partial f}{\partial X_i}\right)^2 \sigma_{X_i}^2 + \sum_{i=1}^{n}\sum_{j=1}^{n} \frac{\partial f^2}{\partial X_i\, \partial X_j} Cov(X_i, X_j) \quad (21)$$

As variance of function Z equals the square of standard deviation of Z, we obtain,

$$\sigma_Z^2 = Var(Z) \quad (22)$$

Using the first-order approximation, the variance of Z is defined as,

$$\sigma_Z^2 = \sum_{i=1}^{n}\left(\frac{\partial f}{\partial X_i}\right)^2 \sigma_{X_i}^2 \quad (23)$$

In present study, it is assumed that the W_0 of a concrete crack in the RC bridge is defined according to Bridge Design Standard (AS 5100.5 – Bridge Design, 2017). The time-dependent concrete crack width is defined as $W_{t_{i,j}}$ with mean and standard deviation under normal distribution. Therefore, the cracking assessment can be analysed based on the difference between $W_{t_{i,j}}$ and W_0. The study of Du et al. (2007) [48] indicates that the reduction in ductility of a RC beam could be significantly affected when the amount of reinforcement corrosion exceeds 10%. Thus, 10% loss of cross-section area of reinforcements is used as the maximum allowable corrosion limit in this study. Hence, the "remaining concrete surface crack width capacity" ($R_{W_{t_{i,j}}}$) and "remaining cross-section area of the corroded steel bars" ($R_{A_{t_{i,j}}}$) can be expressed as,

$$R_{W_{t_{i,j}}} = W_0 - W_{t_{i,j}} = f(X_1, X_2, \dots, X_n)$$

$$R_{A_{t_{i,j}}} = A_0 - A_{t_{i,j}} = f(X_1, X_2, \dots, X_n) \quad (24)$$

Substituting Equations (6), (11) and (12) into Equation (23) leads to,

$$R_{W_{t_{i,j}}} = W_0 - \sum_{i=0,j=0}^{p} (\beta_{i,j} W_{t-i,j} + \varepsilon_t) * \mathbf{1}_{t_j}$$

$$R_{A_{t_{i,j}}} = A_0 - A_0 * \left\{1 - \int_0^{\infty} \left[(0.046 * \frac{r_1}{d} * \mathbf{1}_{W_{t,1}}) + (0.046 * \frac{r_2}{d} * \mathbf{1}_{W_t,2})\right] dt\right\} \quad (25)$$

where $(X_1, X_2, \dots, X_n)$ are random variables, such as uncertainties of cracking width occurred during data acquisition stage [49]. The change in value of $R_{W_{t_{i,j}}}$ depends on the maintenance intervention cycle period (T_{cycle}). As shown in Figure 2, the probability of the width of the surface crack ($W_{t_{i,j}}$) over its allowable value (W_0) as well as the cross-section area of a steel bar ($A_{t_{i,j}}$) over its allowable value (A_0) can be defined as [50],

$$PoF_W = P\left(W_0 - W_{t_{i,j}} < 0\right) = P(R_{W_{t_{i,j}}} < 0)$$

$$PoF_A = P\left(A_0 - A_{t_{i,j}} < 0.90A_0\right) = P(R_{A_{t_{i,j}}} < 0) \quad (26)$$

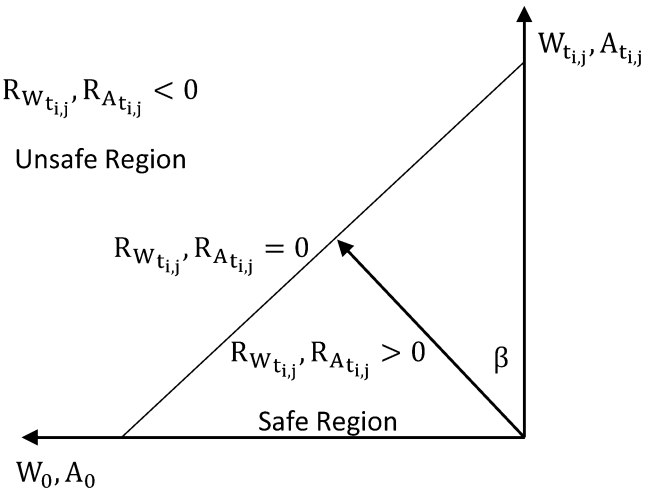

274

275 Figure 4 – Schematic diagram of reliability index.

276 As shown in Figure 4, the minimum distance from origin to the failure line is β which represents

277 the maximum value of PoF [51]. The point $(R_{W_{t_{i,j}}}, R_{A_{t_{i,j}}} = 0)$ represents the design point. Thus,

278 $$\mu_{R_{W_{t_{i,j}}}} = \mu_{W_0} - \mu_{W_{t_{i,j}}}$$

279 $$\mu_{R_{W_{t_{i,j}}}} = \mu_{W_0 - \sum_{i=0,j=0}^{p} (\beta_{i,j} W_{t-i,j} + \varepsilon_t) * \mathbf{1}_{t_j}} \quad (27)$$

280 $$\sigma_{R_{W_{t_{i,j}}}} = \sqrt{\sigma_{W_0}^2 + \sigma_{W_{t_{i,j}}}^2}$$

281

282 $$\mu_{R_{A_{t_{i,j}}}} = \mu_{A_0} - \mu_{A_{t_{i,j}}}$$

283 $$\mu_{R_{A_{t_{i,j}}}} = \mu_{A_0 - A_0 * \left\{1 - \int_0^{\infty} \left[(0.046 * \frac{r_1}{d} * \mathbf{1}_{W_{t,1}}) + (0.046 * \frac{r_2}{d} * \mathbf{1}_{W_{t,2}}) \right] dt \right\}} \quad (28)$$

284 $$\sigma_{R_{A_{t_{i,j}}}} = \sqrt{\sigma_{A_0}^2 + \sigma_{A_{t_{i,j}}}^2}$$

285 where $\mu_{W_{t_{i,j}}}$ and $\sigma_{R_{W_{t_{i,j}}}}$ are the mean and standard deviation of surface crack width, respectively.

286 $\mu_{R_{A_{t_{i,j}}}}$ and $\sigma_{R_{A_{t_{i,j}}}}$ are the mean and standard deviation of cross-section area of the corroded steel

bars, respectively. Hence, engineering β of crack width and cross-section area of the corroded steel bars can be determined as,

$$\beta_{W_{t_{i,j}}} = \frac{\mu_{R_{W_{t_{i,j}}}}}{\sigma_{R_{W_{t_{i,j}}}}} \tag{29}$$

$$\beta_{A_{t_{i,j}}} = \frac{\mu_{R_{A_{t_{i,j}}}}}{\sigma_{R_{A_{t_{i,j}}}}}$$

In addition, the PoF of crack width and cross-section area of the corroded steel bars can be defined as,

$$PoF_W = 1 - \emptyset\left(\beta_{W_{t_{i,j}}}\right) \tag{30}$$

$$PoF_A = 1 - \emptyset\left(\beta_{A_{t_{i,j}}}\right)$$

where Φ () is the cumulative distribution function of a standard normal random variable. The First Order Second Moment (FOSM) is widely used to analyze the load and resistance of the bridges [52]. As shown in Equation (28), the reliability index (β) is defined based on the allowable crack width and reduction in the cross-sectional area of a steel bar (AS 5100.5 – Bridge Design, 2017). As the first estimate, the relationship between the loading imposed on the bridge and the concrete cracking is ignored in this study.

3. Problem description

The developed ERA-based framework was implemented to conduct life-cycle condition assessment of a RC highway bridge (Long Feng Xi Bridge, Chongqing, China) based on the historical inspection data of concrete surface crack width (Figure 5a). The present study mainly

focuses on the No. 4 span of the bridge as shown in Figure 5 b-c. The developments of the 3 cracks have been regularly monitored, and the image of the cracks are shown in Figure 5 d and e. The historical crack width data collected from 2011 to 2018 by Chongqing Expressway Group Company Ltd. were statistically analysed, and the long-term crack development was predicted using the AR model based on W_0 = 0.25 mm (AS 5100.5 – Bridge Design, 2017). In this study, the relationship between the chloride penetration profile, corrosion rate of reinforcement and crack width was established based on Fick's 2nd law and mathematical model which ignores the variation of environment condition. To cater for the effects of different environmental conditions, a series of parametric studies were carried out to investigate the impact of reinforcement corrosion rate on the residual life of the bridge under normal and costal environments, respectively. The experimental studies of [53] revealed that the corrosion rate of steel bars is dependent on the experimental conditions*, i.e.* (1) the value of steel corrosion rate is r_1 under non-exposed-to-air conditions ($W_t \leq W_1$) and (2) the value of steel corrosion rate is r_2 under exposed-to-air conditions ($W_t > W_1$). Although day-night cycles, seasonal cycles, rain periods and extreme temperature cycles could affect the corrosion rate of steel bars in practice [54], it is assumed that the experimental conditions remain constant to simplify the complex corrosion processes in this study. Based on AS 5100.5 – Bridge Design (2017) and previous studies [53, 54], the W_0 (AS 5100.5 – Bridge Design 2017), diffusion coefficient and corrosion rates [55-58] are shown in Table 1.

(a)

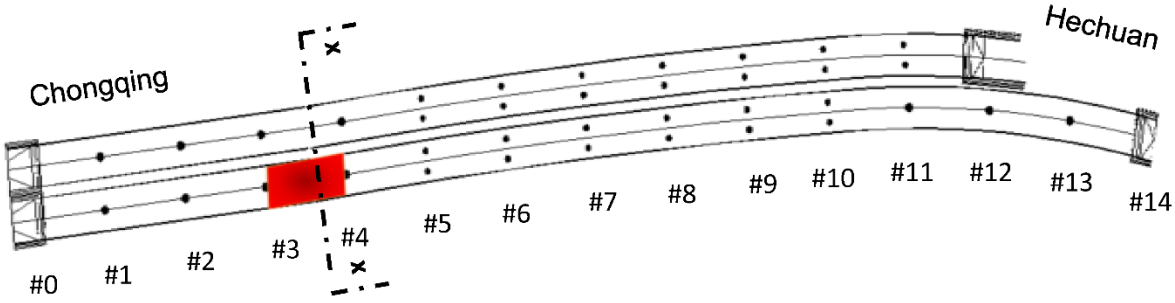
Chongqing
Hechuan
#0
#1
#2
#3
#4
#5
#6
#7
#8
#9
#10
#11
#12
#13
#14

(b)

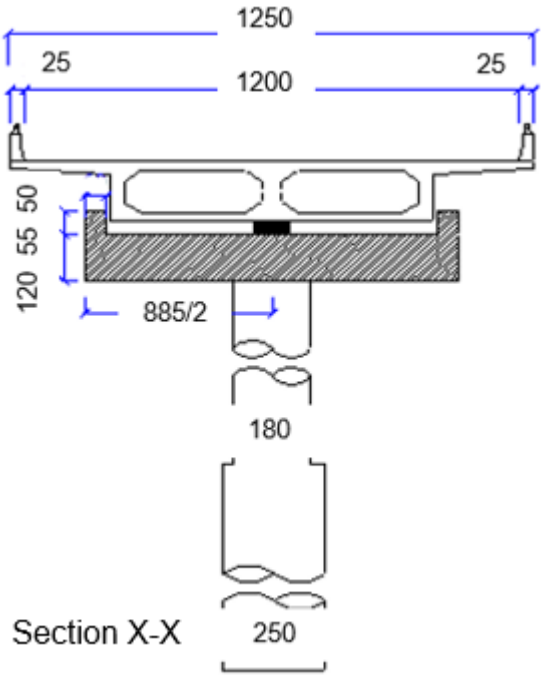
1250
25
1200
25
50
55
120
885/2
180
Section X-X
250

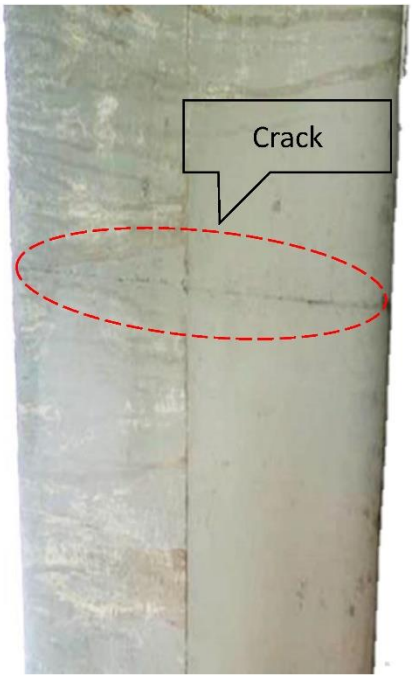
Crack

(c) (d)

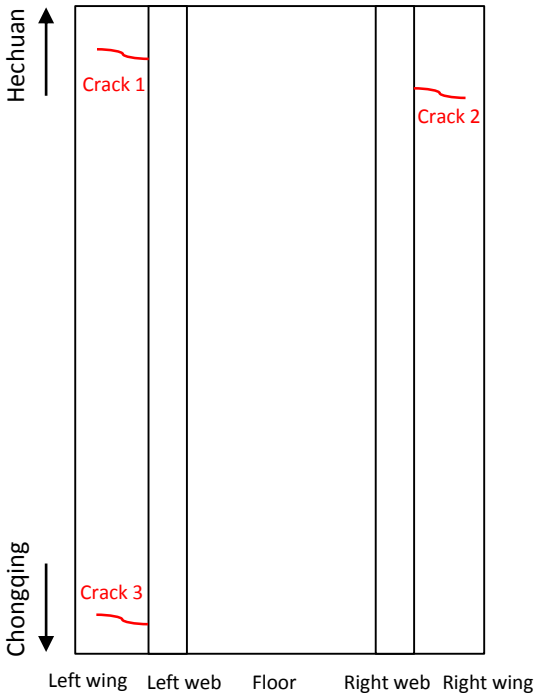

(e)

Figure 5 – Case study of Long Feng Xi Bridge, Chongqing, China: (a) bridge appearance, (b) section of the bridge with cracking investigated in this study, (c) the cross-section X-X, (d) cracking 1 detail and (e) cracks' locations on No.4 span of the bridge.

Table 1 – Value of crack width W_1 causing steel bars exposed to air, different diffusion coefficients of chloride ions in concrete subject to different environmental conditions [55-58] and corrosion rates r_1 and r_2 of a reinforcement steel bar under normal and coastal environmental conditions in this study [53, 54].

Classification of assessment conditions	**W_1 (mm)**	**D_1: $W_t < W_1$ (mm^2/year)**	**D_2: $W_t \geq W_1$ (mm^2/year)**	**r_1: $W_t < W_1$ ($\mu A/cm^2$)**	**r_2: $W_t \geq W_1$ ($\mu A/cm^2$)**
Normal environmental conditions	0.1	63.08	189.24	0.5	2
Coastal environmental conditions	0.1	167.78	503.31	1	10

4. Results and discussions

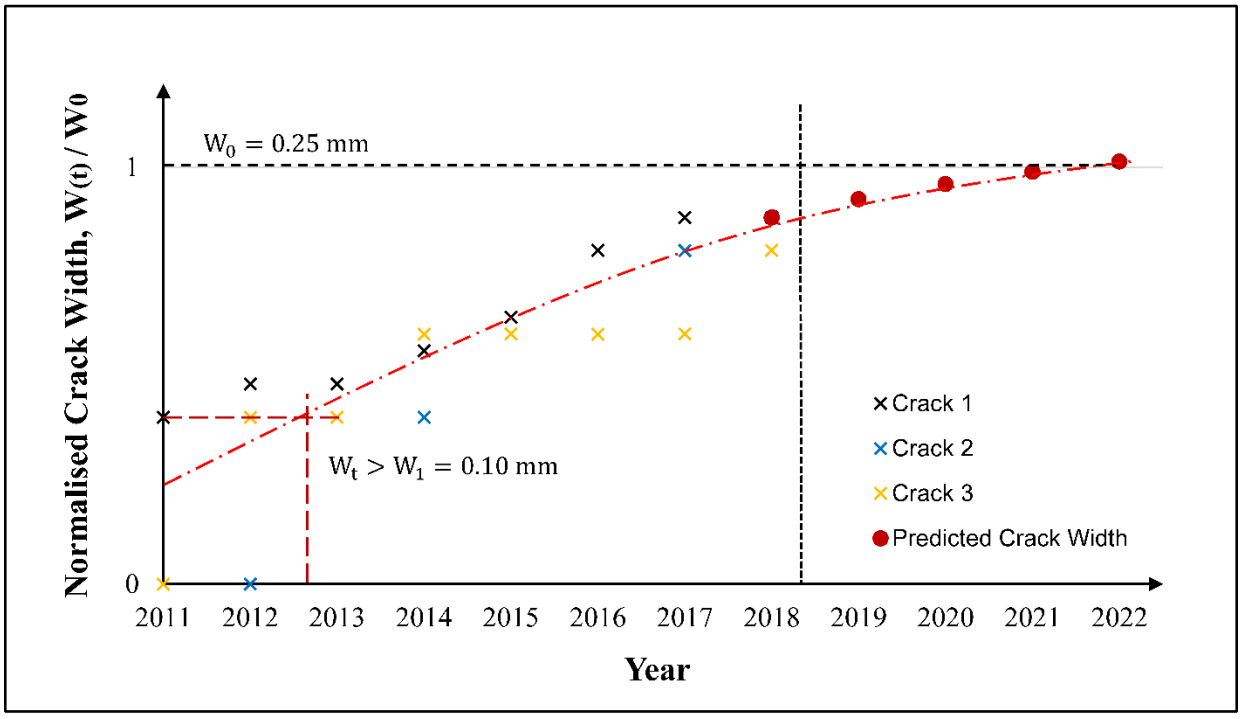

(a)

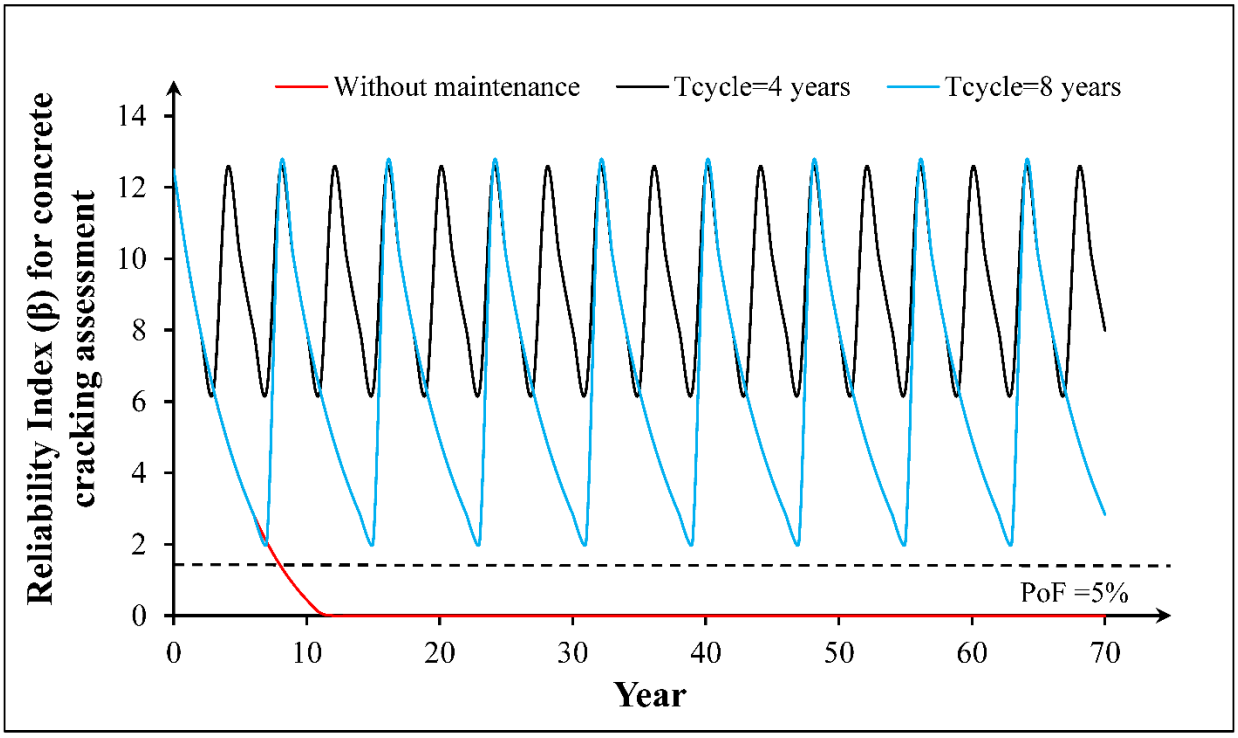

(b)

Figure 6 – (a) Time-dependent normalised crack width prediction using autoregression with 3 cracks data on the same span of bridge, W_0: maximum allowable crack width (AS 5100.5 – Bridge Design, 2017); (b) time-dependent reliability index (β) for concrete cracking assessment under different maintenance intervention cycle periods (T_{cycle}). PoF, probability of failure.

As shown in Figure 6 (a), the long-term crack width is predicted using an autoregression approach based on the available eight-year crack width measurements of 3 different cracks obtained from routine bridge inspection. The model coefficients were determined based on the measurement data using a well-established methodology proposed by Hagan et al (1987) [31]. The linear crack width evolution trend results from the limited historical measurement data. With more crack data available over the time, the prediction of autoregression model will become more accurate. The model predicted that, without any crack repair, the crack width will reach its threshold (i.e. W_0 = 0.25mm, AS 5100.5 - Bridge Design, 2017) between 2021 and 2022. Figure 6 (b) shows the effects of different maintenance intervention cycle periods (T_{cycle}) on the time-dependent β. Assuming PoF ≤ 5% of W_0 is the objective of the road authority, it indicates that the service life of the bridge, in terms of allowable crack width (W_0), is very sensitive to T_{cycle}. For example, the reduction of T_{cycle} by 50% (*i.e.* reduce T_{cycle} from 8 years to 4 years) could lead to three-fold increase of β, and therefore prolong the time for crack width to reach its allowable value. However, without a maintenance plan, the time for the crack width to reach W_0 would be significantly shortened (*i.e.* less than 10 years).

Although the surface crack of the bridge can be fixed through regular maintenance, the chloride penetration and corrosion of the steel bars in concrete will continue over time with certain diffusion coefficient and corrosion rate which are dependent on different maintenance intervention cycle periods (T_{cycle}). Figure 7a shows that chloride content at 50 mm depth in concrete increases with time because of the chloride penetration even the crack is sealed. Meanwhile, because the diffusion coefficient D is larger when concrete crack width W_t is greater than W_1 (0.1mm), the

382 figure 7a shows different chloride profiles under different maintenance intervention cycles. In
383 figure 7b, assuming the allowable loss of the cross-section of a steel bar is 10% (i.e. $A_t/A_0 \geq 90\%$),
384 the time-dependent normalised cross-section area of a steel bar ($A_t/A_0 \geq 90\%$) under different
385 T_{cycle} is shown, while the time-dependent value of β under different T_{cycle} can be found in Figure
386 7c. It demonstrates that reducing T_{cycle} from 12 years to 4 years could prolong the service life of
387 the bridge by around 15 years. In addition, assuming PoF ≤ 5% loss of cross-section area of a
388 steel bar is the objective of the road authority, the maintenance intervention cycle period of (T_{cycle})
389 should be 4 years to prolong the service life to 70 years from a conservative perspective.

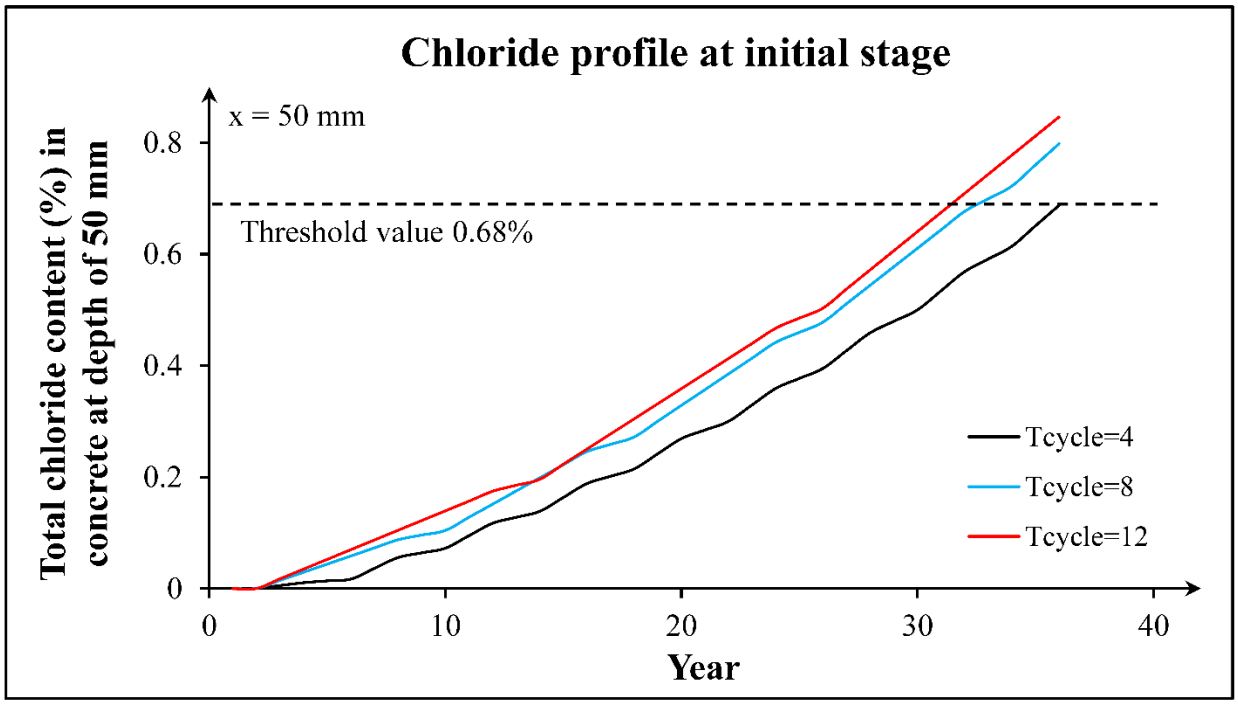

390

391 (a)

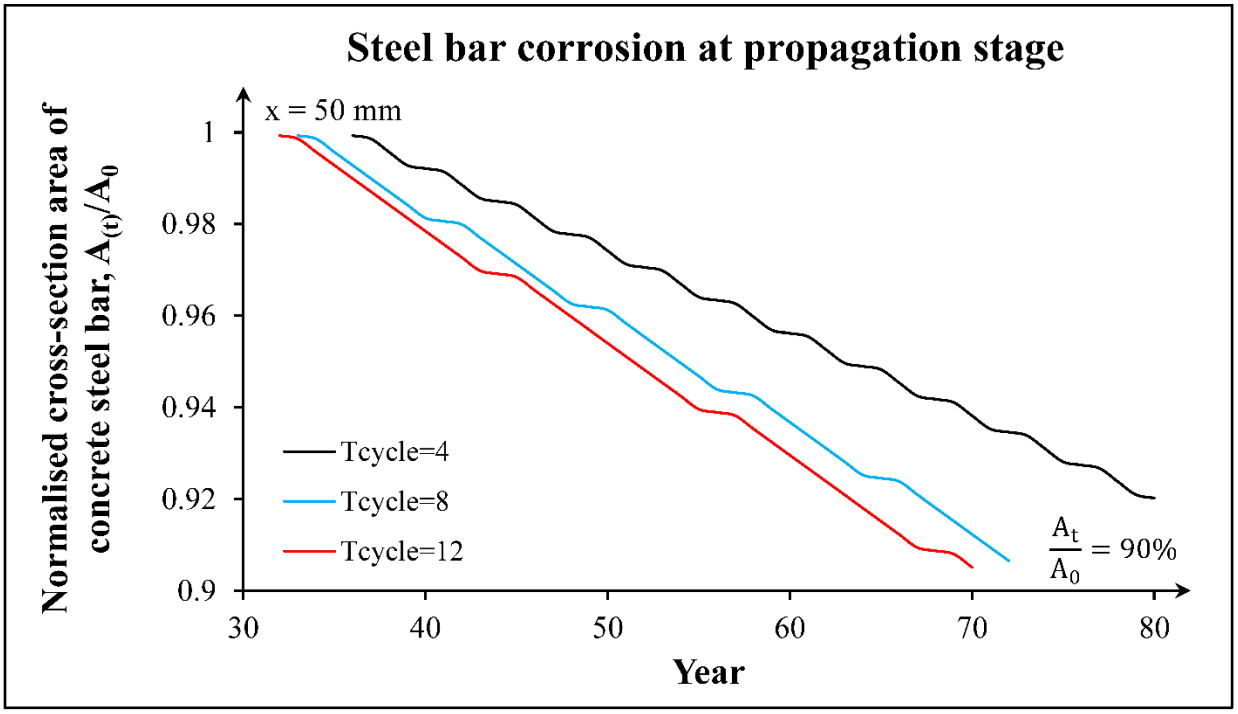
Steel bar corrosion at propagation stage
x = 50 mm
Normalised cross-section area of concrete steel bar, $A_{(t)}/A_0$
1
0.98
0.96
0.94
0.92
0.9
30
40
50
60
70
80
Year
Tcycle=4
Tcycle=8
Tcycle=12
$\frac{A_t}{A_0}$ = 90%

(b)

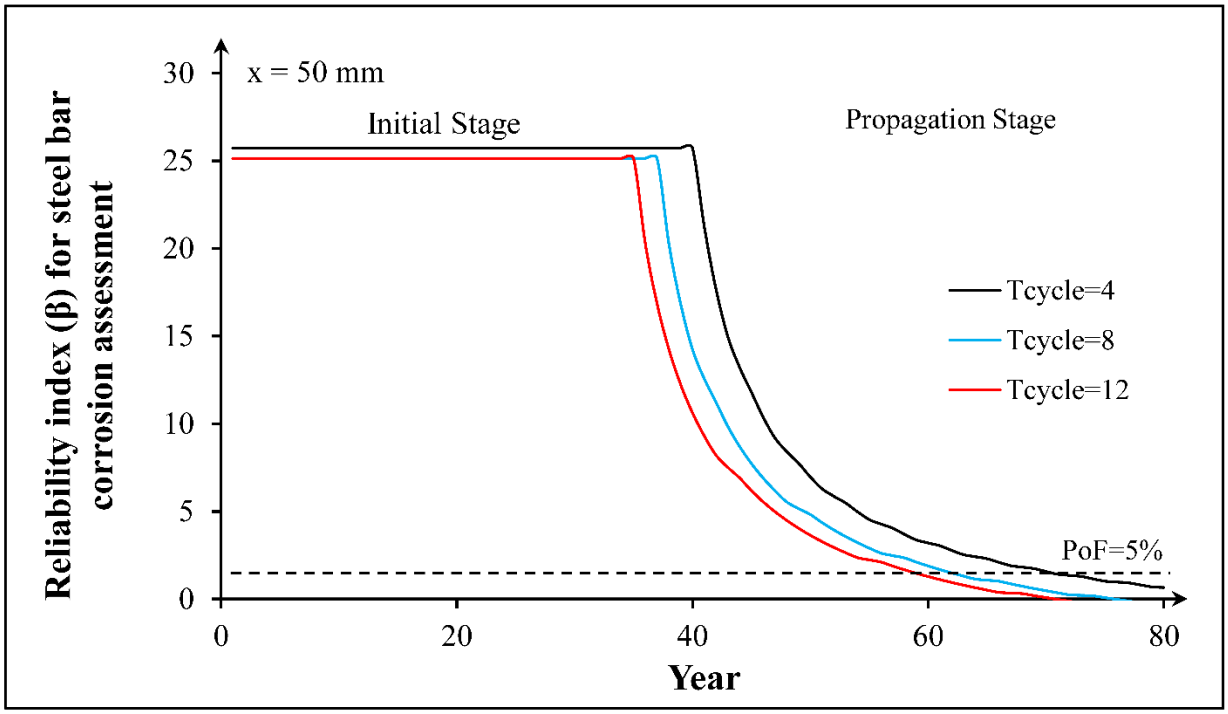
x = 50 mm
Initial Stage
Propagation Stage
Reliability index (β) for steel bar corrosion assessment
30
25
20
15
10
5
0
0
20
40
60
80
Year
Tcycle=4
Tcycle=8
Tcycle=12
PoF=5%

(c)

Figure 7 - (a) Chloride profile of total chloride content in concrete at depth 50 mm at initial stage; (b) Time-dependent normalised cross-section area of concrete steel bar prediction using steel corrosion model at propagation stage; (c) time-dependent reliability index (β) for steel bar corrosion assessment under different maintenance intervention cycle periods (T_{cycle}). PoF, probability of failure.

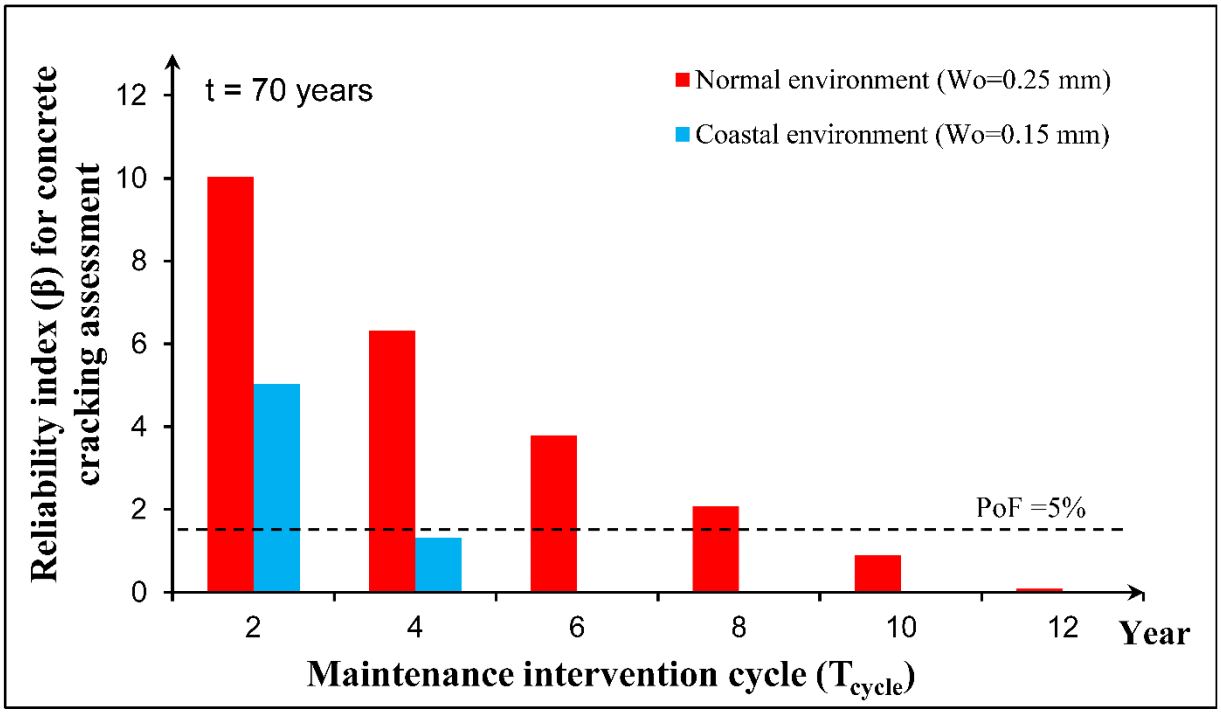

(a)

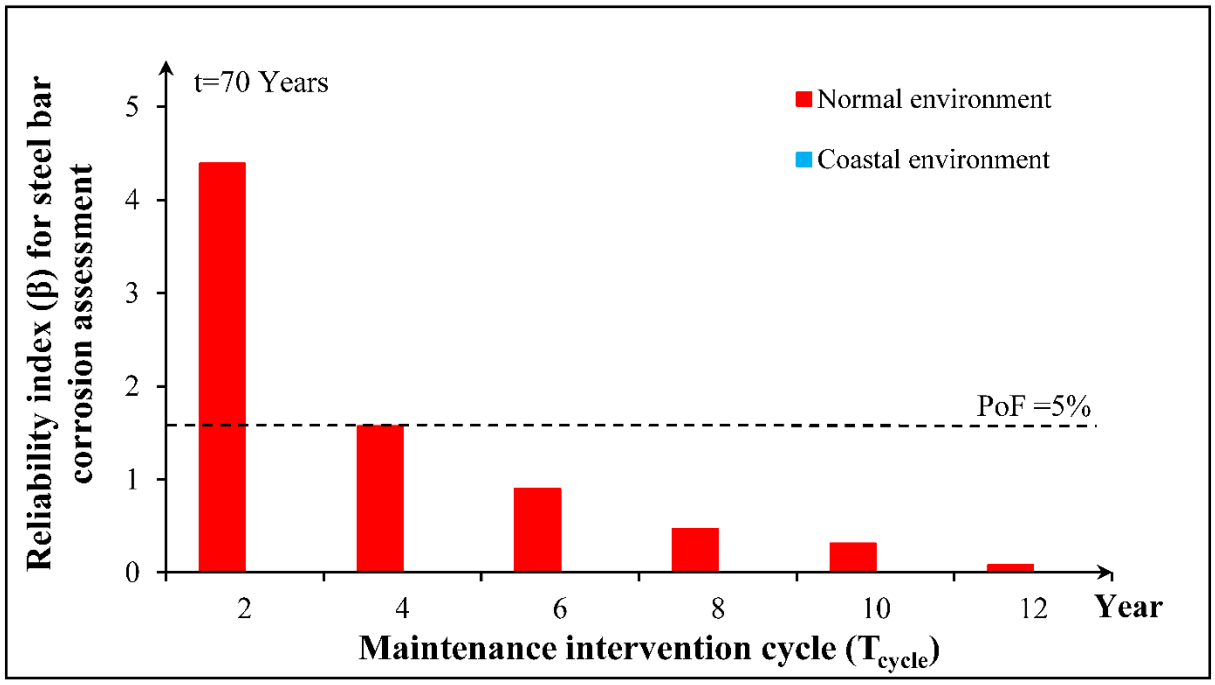

(b)

Figure 8 – (a) Reliability index (β) for concrete cracking assessment at t = 70 years under different maintenance intervention cycle periods (T_{cycle}) and different environmental conditions (normal environment: W_0 = 0.25 mm; coastal environment: W_0 = 0.15 mm); (b) reliability index (β) for steel bar corrosion assessment at t = 70 years under different maintenance intervention periods T_{cycle} and different environmental conditions (normal environment: W_0 = 0.25 mm; coastal environment: W_0 = 0.15 mm). PoF, probability of failure.

Figure 8 shows ERA assessment results of concrete cracking and steel bar corrosion of Long Feng Xi Bridge at t = 70 years under normal and coastal environmental conditions. It can be seen from Figure 8a that for concrete crack assessment, T_{cycle} should be 8 years and 2 years for normal and coastal environmental conditions, respectively. In addition, for steel bar corrosion assessment, T_{cycle} should be 2 years for normal environmental conditions from a conservative perspective. However, in costal environmental condition the corrosion causes serious rate of damage of structure even the T_{cycle} is 2 years. Since the reliability index is below the target value.

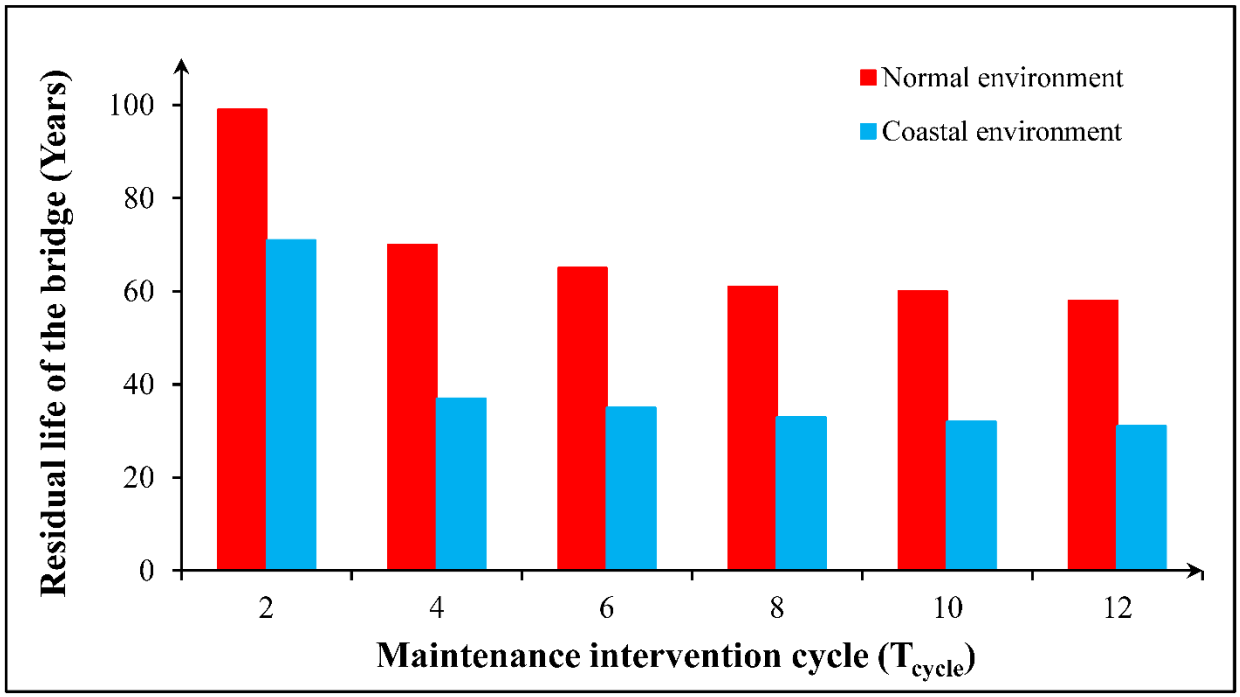

Figure 9 – Estimated residual life of Long Feng Xi Bridge, Chongqing, China, with 5% probability of failure under different maintenance intervention cycle periods (T_{cycle}) and under two different environmental conditions.

Based on the historical cracking data, the ERA-based framework can be implemented to predict the residual life of a bridge. As shown in Figure 9, the residual life of a bridge is sensitive to the external environmental conditions. Under along maintenance intervention cycle period (e.g. T_{cycle} = 6 years), the residual life of the bridge under normal environmental conditions is 2 times longer than that under coastal environmental conditions. However, the difference of the residual life of the bridge under normal and coastal environmental conditions can be significantly reduced with a short intervention cycle period (e.g. T_{cycle} = 2 years).

5. Conclusion

The present study investigated the concrete crack induced corrosion of steel bars by developing ERA-based model using the eight-year inspection data from 3 different cracks of an operating bridge. The following are some major conclusions:

- The residual service life of a RC bridge based on the allowable crack width (W_0) is dependent on the maintenance intervention cycle period (T_{cycle}). To make sure the PoF of surface crack width is less than 5%, the T_{cycle} should be reduced by 65% (i.e. change T_{cycle} from 12 years to 4 years) which could lead to three-fold increase of β, and therefore prolong the service life of a bridge.
- Even if the surface crack of a RC bridge is repairable through periodic maintenance, the corrosion of the steel bars in the bridge could continue over time with a corrosion rate which depends on different T_{cycle}. It shows that reducing T_{cycle} from 12 years to 4 years could prolong the service life of the bridge by around 15 years.
- To make sure the probability of failure of the cross-section area of a steel bar is less than 5%, T_{cycle} should be less than 4 years to prolong the service life to 70 years.
- T_{cycle} of a RC bridge is very sensitive to its external environment. To fulfil the allowable surface crack requirement, T_{cycle} should be 8 years and 2 years for bridges under normal and coastal environmental conditions, respectively. To fulfil the allowable steel bar corrosion requirement, T_{cycle} should be at least 2 years for bridges under both normal and coastal environmental conditions.
- Under coastal environmental conditions, the maintenance intervention cycle period needs to be significantly shortened to prolong the service life to 70 years (e.g. T_{cycle} = 2 years).

It should be mentioned that the reliability-based model developed in this study is completely general and are not in any way particular to a specific type of bridges. Sustainability assessment of concrete bridges under extreme environmental conditions is of critical importance all around the world [59]. However, much work is still to be done to accurately establish the correlation

between the reinforcement corrosion and crack development in concrete. Using a RC bridge in Chongqing, China as a case study, the present study could contribute to the accurate prediction of reinforcement corrosion induced by concrete cracking.

Limitations

It should be mentioned that the relationship between the diffusion coefficient, corrosion rate of reinforcement and crack width was established based on previous literatures which ignores the variation of real environment condition. In addition, the traffic load induced concrete cracking was not considered in this study. Our future research will address these limitations and focus on model validation by collecting more bridge inspection data.

ACKNOWLEDGEMENTS

The authors wish to thank the Australian Research Council (ARC IH150100006), CRC Bushfire & Natural Hazards, and The University of Melbourne for their support.

References

[1] X. Tong, H. Yang, L. Wang, Y. Miao, The development and field evaluation of an IoT system of low-power vibration for bridge health monitoring, Sensors 19(5) (2019) 1222.

[2] M. Sanchez-Silva, G.-A. Klutke, D.V. Rosowsky, Life-cycle performance of structures subject to multiple deterioration mechanisms, Structural Safety 33(3) (2011) 206-217.

[3] S. Jamali, T.H. Chan, A. Nguyen, D.P. Thambiratnam, Reliability-based load-carrying capacity assessment of bridges using structural health monitoring and nonlinear analysis, Structural Health Monitoring 18(1) (2019) 20-34.

[4] H. Kim, E. Ahn, M. Shin, S.-H. Sim, Crack and noncrack classification from concrete surface images using machine learning, Structural Health Monitoring 18(3) (2019) 725-738.

[5] S. Yehia, O. Abudayyeh, S. Nabulsi, I.J.J.o.B.E. Abdelqader, Detection of common defects in concrete bridge decks using nondestructive evaluation techniques, 12(2) (2007) 215-225.

[6] L. Zhang, P. Mendis, W.C. Hon, S. Fragomeni, N. Lam, Y. Song, Effects of cyclic loading on the long-term deflection of prestressed concrete beams, COMPUTERS AND CONCRETE 12(6) (2013) 739-754.

[7] C.G. Koh, K.K. Ang, L. Zhang, Effects of repeated loading on creep deflection of reinforced concrete beams, ENGINEERING STRUCTURES 19(1) (1997) 2-18.

[8] P.D. Krauss, E.A. Rogalla, Transverse cracking in newly constructed bridge decks, 1996.
[9] Y. Du, L. Clark, A. Chan, Residual capacity of corroded reinforcing bars, Magazine of Concrete Research 57(3) (2005) 135-147.
[10] K.G. Papakonstantinou, M. Shinozuka, Probabilistic model for steel corrosion in reinforced concrete structures of large dimensions considering crack effects, Engineering Structures 57 (2013) 306-326.
[11] D. Sun, H. Shi, K. Wu, S. Miramini, B. Li, L. Zhang, Influence of aggregate surface treatment on corrosion resistance of cement composite under chloride attack, Construction and Building Materials 248 (2020) 118636.
[12] D. Sun, K. Wu, H. Shi, L. Zhang, L. Zhang, Effect of interfacial transition zone on the transport of sulfate ions in concrete, Construction and Building Materials 192 (2018) 28-37.
[13] D. Sun, K. Wu, H. Shi, S. Miramini, L. Zhang, Deformation behaviour of concrete materials under the sulfate attack, Construction and Building Materials 210 (2019) 232-241.
[14] L.A. Abo Alarab, A. Poursaee, B.E. Ross, An experimental method for evaluating reinforcement corrosion in cracked concrete, Journal of Structural Integrity and Maintenance 4(1) (2019) 43-50.
[15] L. Chernin, D.V. Val, K.Y. Volokh, Analytical modelling of concrete cover cracking caused by corrosion of reinforcement, Materials and Structures 43(4) (2010) 543-556.
[16] C. Alonso, C. Andrade, J. Rodriguez, J.M. Diez, Factors controlling cracking of concrete affected by reinforcement corrosion, Materials and structures 31(7) (1998) 435-441.
[17] L. Chun-Qing, R.E. Melchers, Z. Jian-Jun, Analytical model for corrosion-induced crack width in reinforced concrete structures, ACI Materials Journal 103(4) (2006) 479.
[18] F. Molina, C. Alonso, C. Andrade, Cover cracking as a function of rebar corrosion: Part 2—Numerical model, Materials and structures 26(9) (1993) 532-548.
[19] Y. Du, A. Chan, L. Clark, Finite element analysis of the effects of radial expansion of corroded reinforcement, Computers & structures 84(13-14) (2006) 917-929.
[20] A.A. Torres-Acosta, M. Mart ı´ nez-Madrid, Residual life of corroding reinforced concrete structures in marine environment, Journal of Materials in Civil Engineering 15(4) (2003) 344-353.
[21] C.-Q. Li, S. Yang, Prediction of concrete crack width under combined reinforcement corrosion and applied load, Journal of engineering mechanics 137(11) (2011) 722-731.
[22] M.-T. Liang, R. Huang, S.-A. Feng, C.-J. Yeh, Service life prediction of pier for the existing reinforced concete bridges in chloride-laden environment, Journal of Marine Science and Technology 17(4) (2009) 312-319.
[23] Q. Pan, D. Dias, An efficient reliability method combining adaptive support vector machine and Monte Carlo simulation, Structural Safety 67 (2017) 85-95.
[24] M.G. Stewart, D.V. Rosowsky, Time-dependent reliability of deteriorating reinforced concrete bridge decks, Structural safety 20(1) (1998) 91-109.
[25] K.A.T. Vu, M.G. Stewart, Time-dependent reliability of deteriorating reinforced concrete bridge decks, Structural Safety 22(4) (2000) 313-333.
[26] F. Akgül, D.M. Frangopol, Time-dependent interaction between load rating and reliability of deteriorating bridges, Engineering Structures 26(12) (2004) 1751–1765.
[27] D.V. Val, R.E. Melchers, Reliability of deteriorating RC slab bridges, Journal of Structural Engineering 123(12) (1997) 1638-1644.
[28] J. Chakraborty, A. Katunin, Detection of structural changes in concrete using embedded ultrasonic sensors based on autoregressive model, Diagnostyka 20 (2019).
[29] D.V. Val, M.G. Stewart., R.E. Melchers, Effect of reinforcement corrosion on reliability of highway bridges, Engineering Structures 20(11) (1998) 1010-1019.
[30] L. Liao, F. Köttig, Review of hybrid prognostics approaches for remaining useful life prediction of engineered systems, and an application to battery life prediction, IEEE Transactions on Reliability 63(1) (2014) 191-207.

[31] M.T. Hagan, S.M. Behr, The time series approach to short term load forecasting, IEEE Transactions on Power Systems 2(3) (1987) 785-791.
[32] Y. Okazaki, S. Okazaki, S. Asamoto, P.j. Chun, Applicability of machine learning to a crack model in concrete bridges, Computer-Aided Civil and Infrastructure Engineering (2020).
[33] H. Akaike, Fitting autoregressive models for prediction, Annals of the institute of Statistical Mathematics 21(1) (1969) 243-247.
[34] H. Akaike, A new look at the statistical model identification, Selected Papers of Hirotugu Akaike, Springer1974, pp. 215-222.
[35] R. Shibata, Selection of the order of an autoregressive model by Akaike's information criterion, Biometrika 63(1) (1976) 117-126.
[36] O. Poupard, A. Aıt-Mokhtar, P. Dumargue, Corrosion by chlorides in reinforced concrete: Determination of chloride concentration threshold by impedance spectroscopy, Cement and Concrete Research 34(6) (2004) 991-1000.
[37] M. Liang, K. Wang, C. Liang, Service life prediction of reinforced concrete structures, Cement and Concrete Research 29(9) (1999) 1411-1418.
[38] L. Zhang, B.S. Gardiner, D.W. Smith, P. Pivonka, A.J. Grodzinsky, IGF uptake with competitive binding in articular cartilage, Journal of Biological Systems 16(02) (2008) 175-195.
[39] L. Zhang, D.W. Smith, B.S. Gardiner, A.J. Grodzinsky, Modeling the insulin-like growth factor system in articular cartilage, PloS one 8(6) (2013) e66870.
[40] C. Alonso, C. Andrade, M. Castellote, P. Castro, Chloride threshold values to depassivate reinforcing bars embedded in a standardized OPC mortar, Cement and Concrete research 30(7) (2000) 1047-1055.
[41] M. Alonso, M. Sanchez, Analysis of the variability of chloride threshold values in the literature, Materials and Corrosion 60(8) (2009) 631-637.
[42] U.M. Angst, B. Elsener, C.K. Larsen, Ø. Vennesland, Chloride induced reinforcement corrosion: Electrochemical monitoring of initiation stage and chloride threshold values, Corrosion Science 53(4) (2011) 1451-1464.
[43] B. Elsener, C. Andrade, J. Gulikers, R. Polder, M.J.M. Raupach, Structures, Hall-cell potential measurements—Potential mapping on reinforced concrete structures, Materials and Structures 36(7) (2003) 461-471.
[44] E.J. Henley, H. Kumamoto, Reliability engineering and risk assessment, Prentice-Hall Englewood Cliffs (NJ)1981.
[45] S. Mahadevan, A.J.J.W. Haldar, Sons, Probability, reliability and statistical method in engineering design, (2000).
[46] M. Modarres, M.P. Kaminskiy, V. Krivtsov, Reliability engineering and risk analysis: a practical guide, CRC press2016.
[47] R. Rackwitz, Reliability analysis—a review and some perspectives, Structural safety 23(4) (2001) 365-395.
[48] Y. Du, L.A. Clark, A.H. Chan, Impact of reinforcement corrosion on ductile behavior of reinforced concrete beams, ACI Structural Journal 104(3) (2007) 285.
[49] D. Straub, R. Schneider, E. Bismut, H.-J. Kim, Reliability analysis of deteriorating structural systems, Structural Safety 82 (2020) 101877.
[50] Z. Wang, P. Wang, A new approach for reliability analysis with time-variant performance characteristics, Reliability Engineering 115 (2013) 70-81.
[51] C. Cheng, L. Zhang, R.G. Thompson, Disaster waste clean-up system performance subject to time-dependent disaster waste accumulation, Natural Hazards 91(2) (2018) 717-734.
[52] T. García-Segura, V. Yepes, D.M. Frangopol, D.Y. Yang, Lifetime reliability-based optimization of post-tensioned box-girder bridges, Engineering Structures 145 (2017) 381-391.

[53] M. Jaśniok, T. Jaśniok, Evaluation of maximum and minimum corrosion rate of steel rebars in concrete structures, based on laboratory measurements on drilled cores, Procedia engineering 193 (2017) 486-493.
[54] C. Andrade, C. Alonso, J.J. Sarrıa, Corrosion rate evolution in concrete structures exposed to the atmosphere, Cement and concrete composites 24(1) (2002) 55-64.
[55] J. Wu, B. Diao, Y. Ye, X. Zheng, Chloride diffusivity and life prediction of cracked RC beams exposed to different wet-dry ratios and exposure duration, Advances in Materials Science and Engineering 2017 (2017).
[56] B. Šavija, J. Pacheco, E. Schlangen, Lattice modeling of chloride diffusion in sound and cracked concrete, Cement and Concrete Composites 42 (2013) 30-40.
[57] A. Costa, J. Appleton, Chloride penetration into concrete in marine environment-Part II: Prediction of long term chloride penetration, Materials and Structures 32(5) (1999) 354-359.
[58] T. Cheewaket, C. Jaturapitakkul, W. Chalee, Concrete durability presented by acceptable chloride level and chloride diffusion coefficient in concrete: 10-year results in marine site, Materials and Structures 47(9) (2014) 1501-1511.
[59] I.J. Navarro, J.V. Martí, V. Yepes, Reliability-based maintenance optimization of corrosion preventive designs under a life cycle perspective, Environmental Impact Assessment Review 74 (2019) 23-34.

Figure

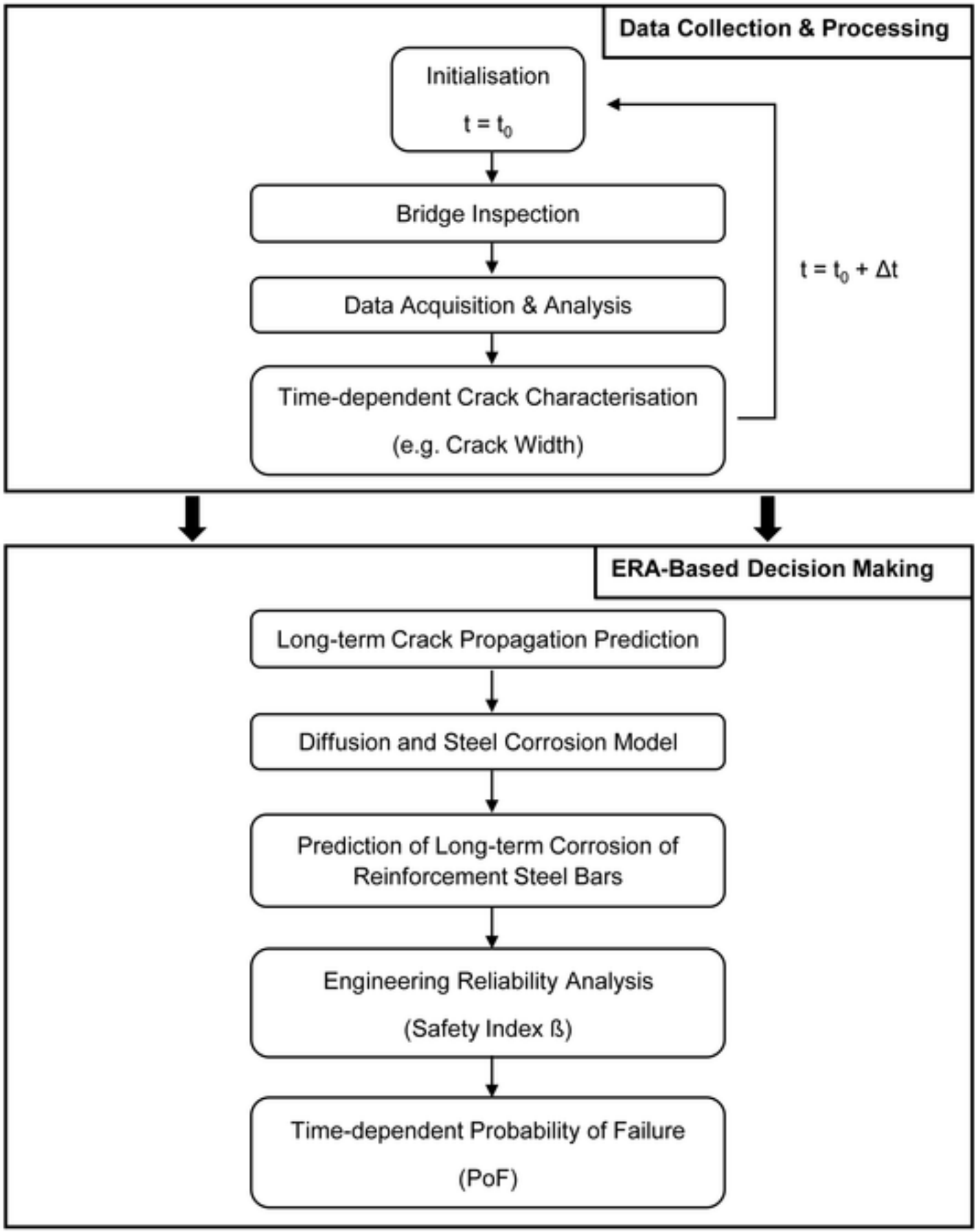

Figure

Click here to access/download;Figure;Figure 2 V3.tiff

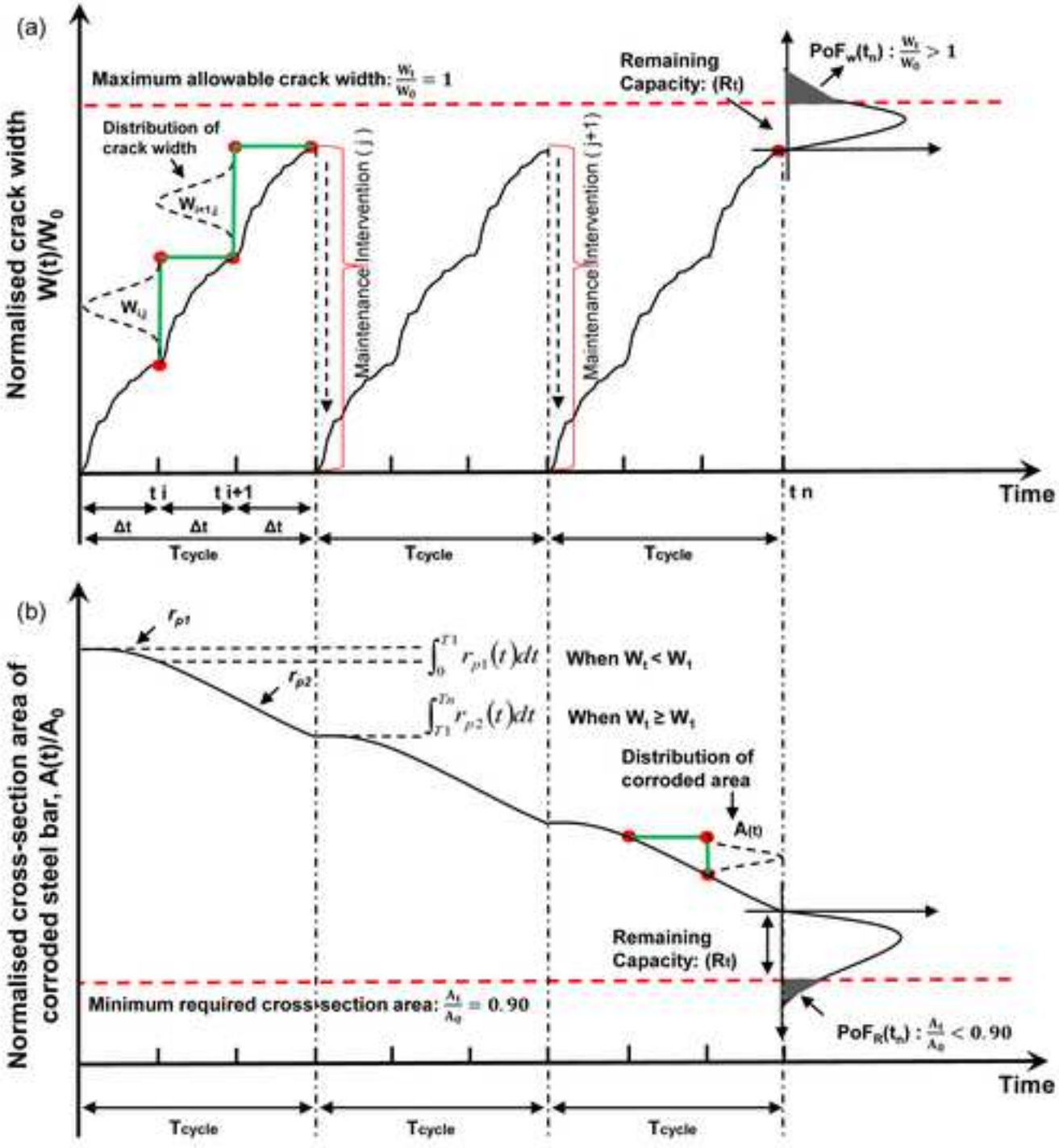

Figure

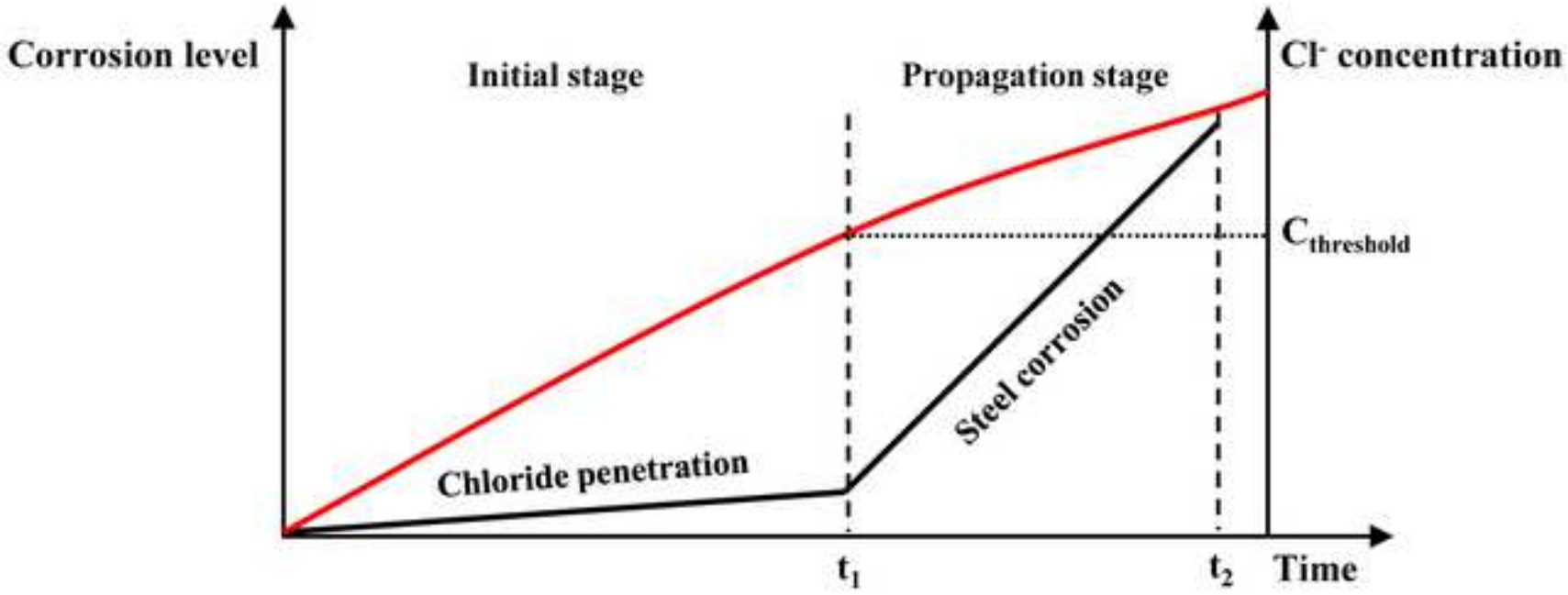

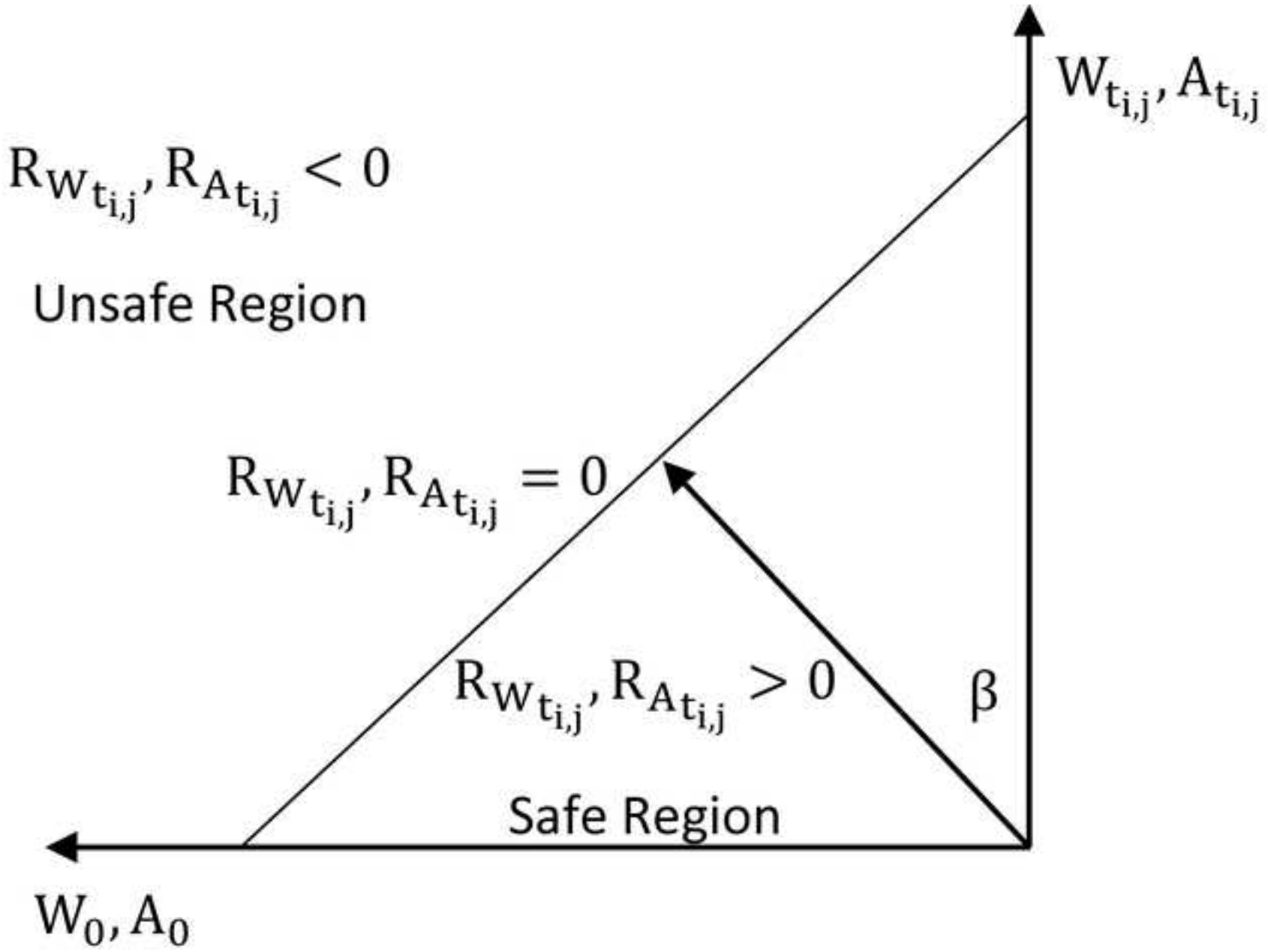

Figure

Click here to access/download;Figure;Figure 5 (a).jpg

Figure

Click here to access/download;Figure;Figure 5 (b).TIF.tiff

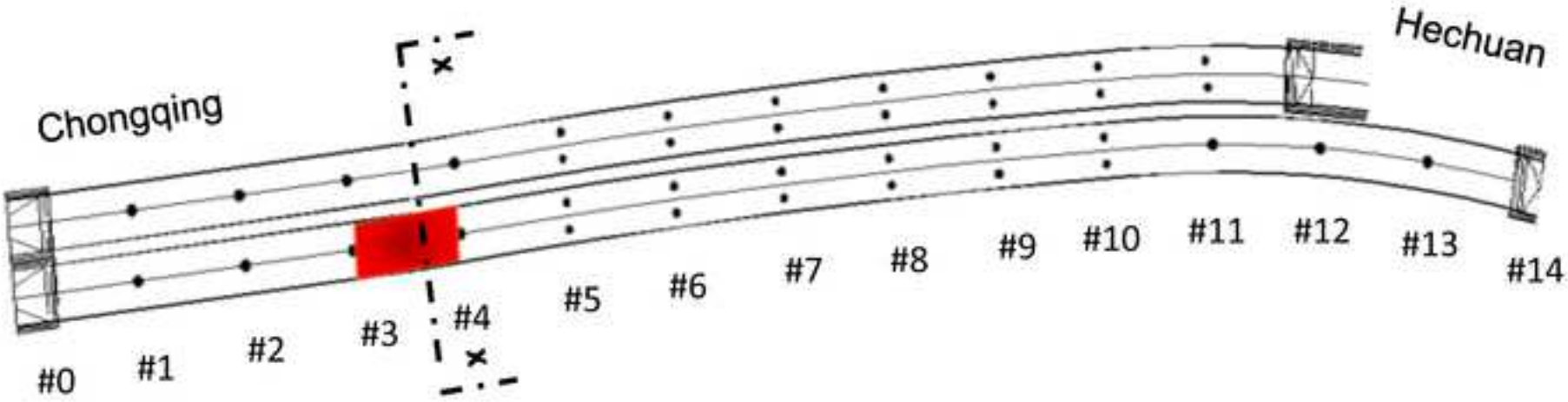

Figure

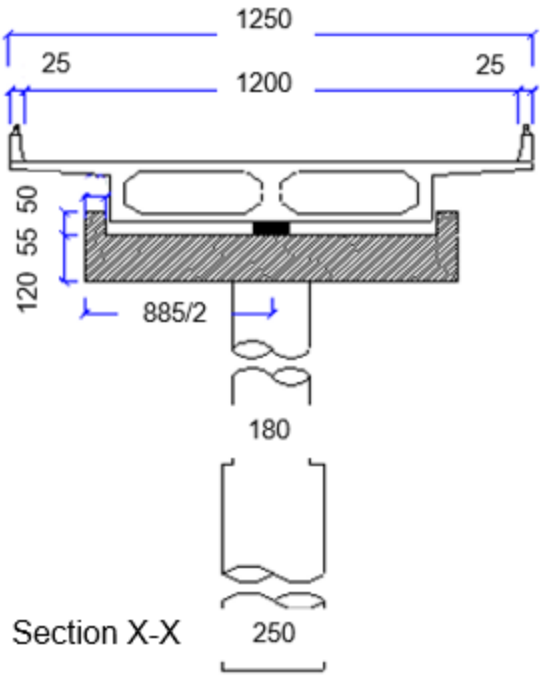

Figure

Click here to access/download;Figure;Figure 5 (d).TIF.tiff

Figure

Click here to access/download;Figure;Figure 5 (e).docx

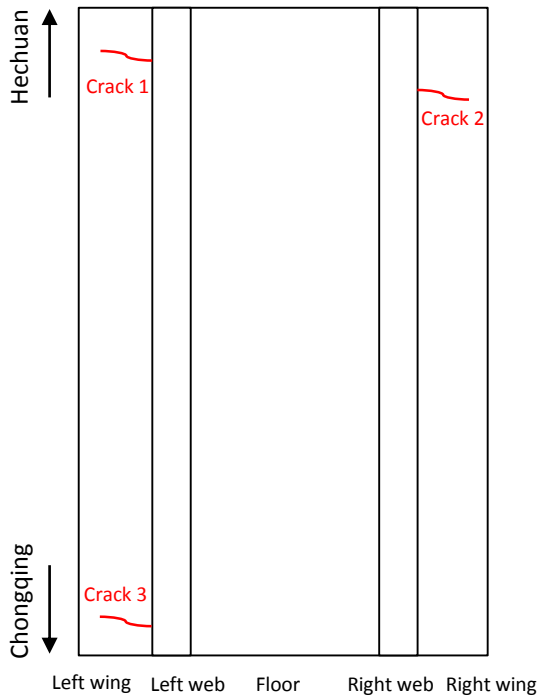

Figure

Click here to access/download;Figure;Figure 6 (a) Update V1.tiff

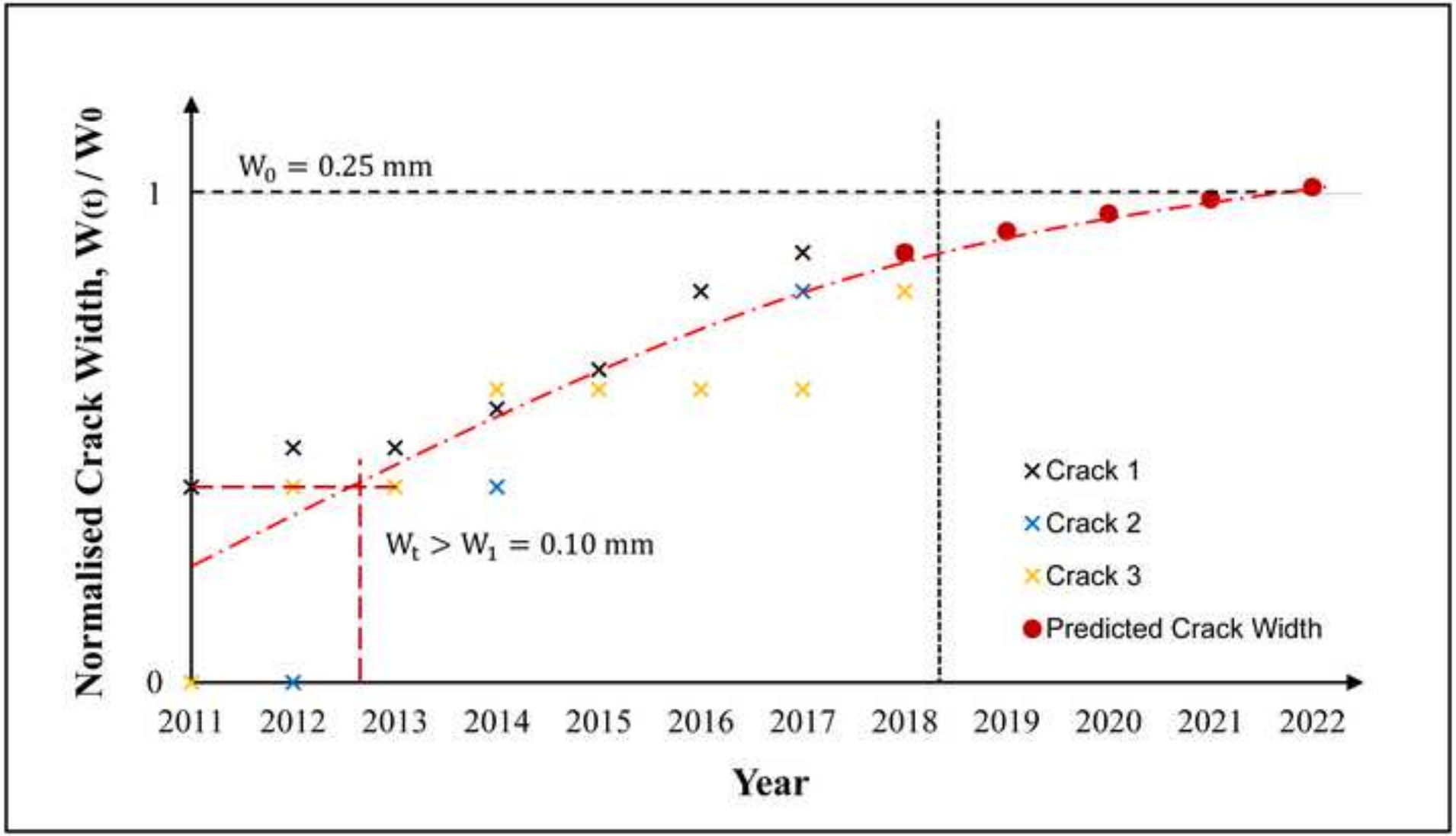

Figure

Click here to access/download;Figure;Figure 6 (b) Update V1.tiff

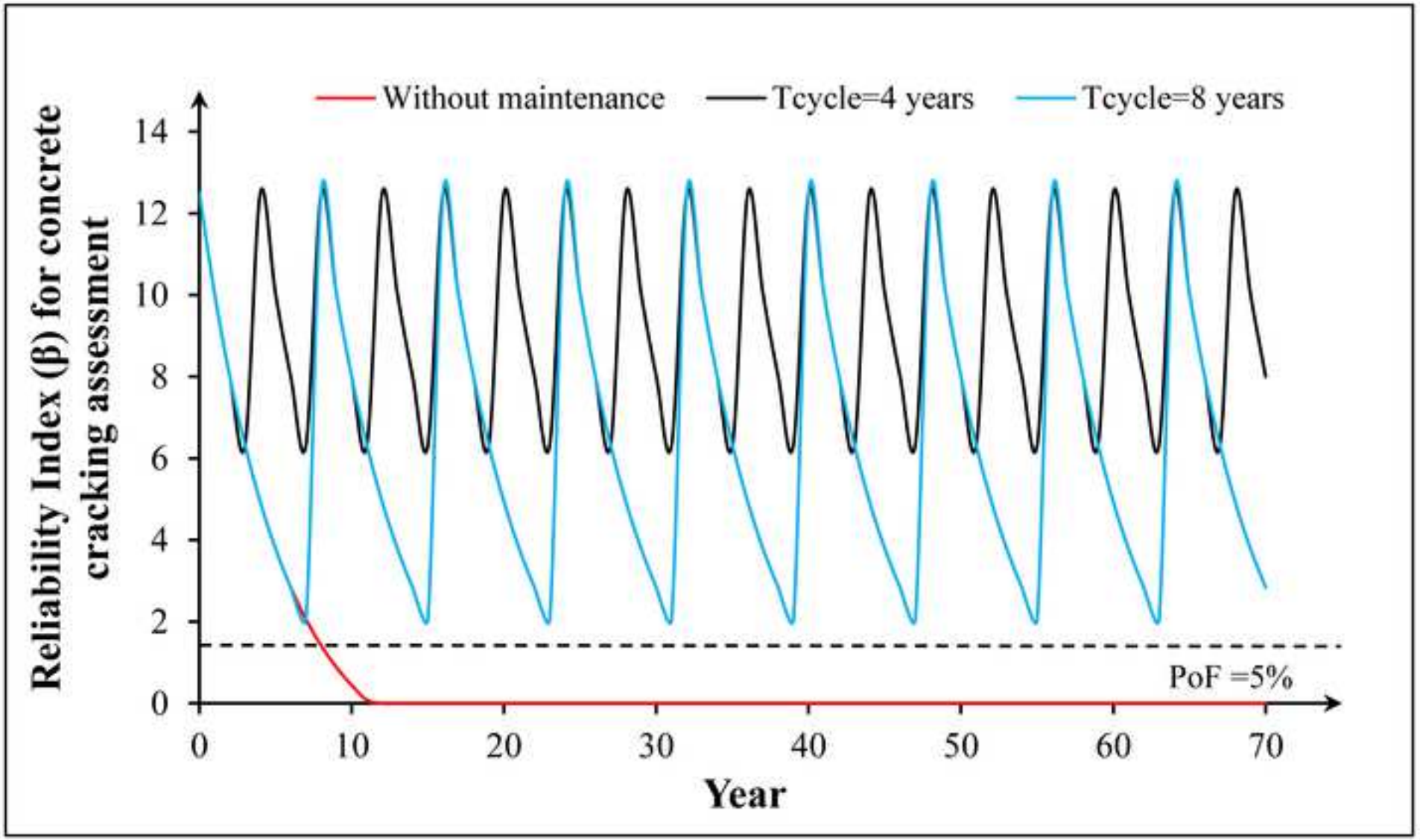

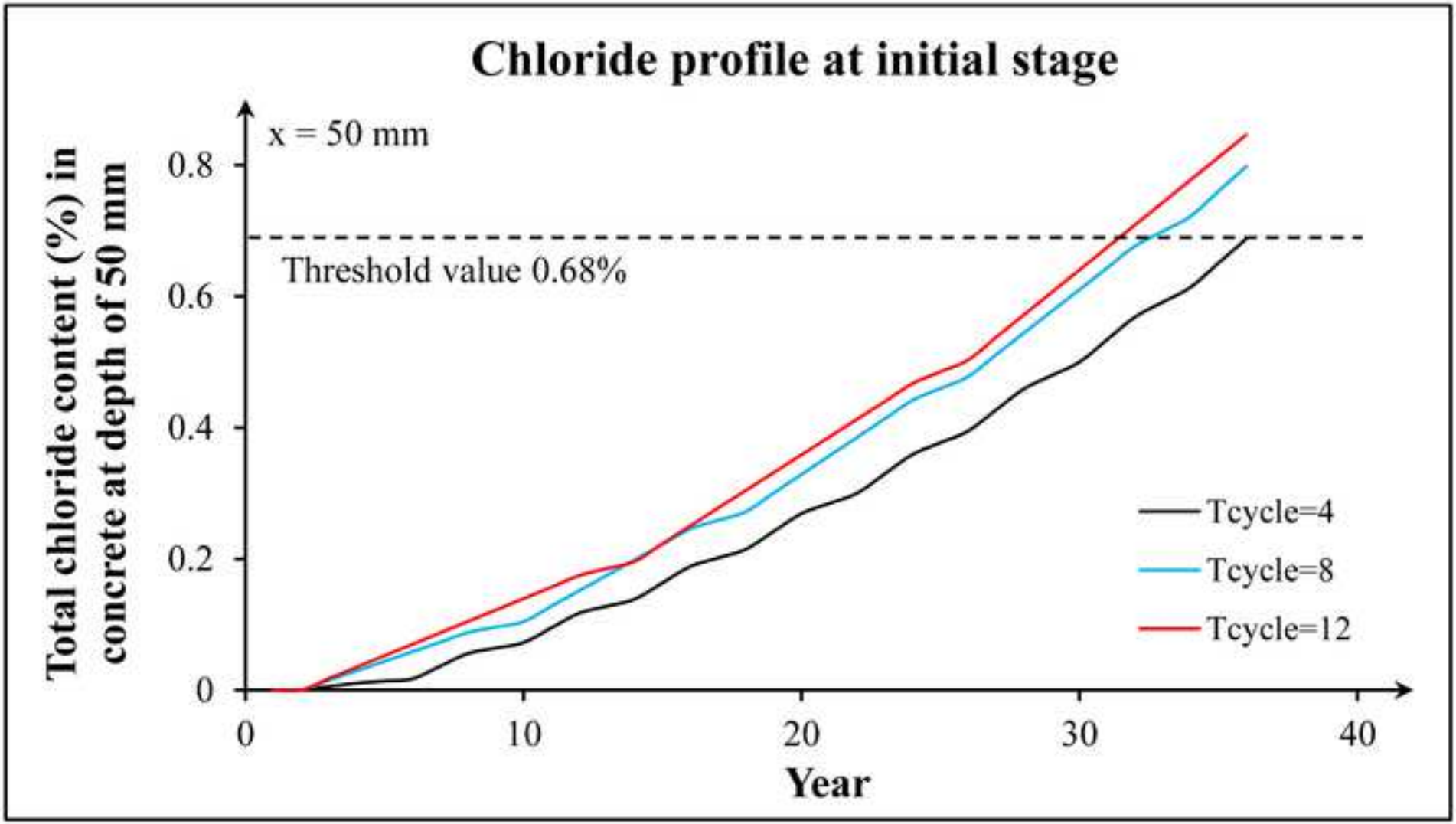

Figure

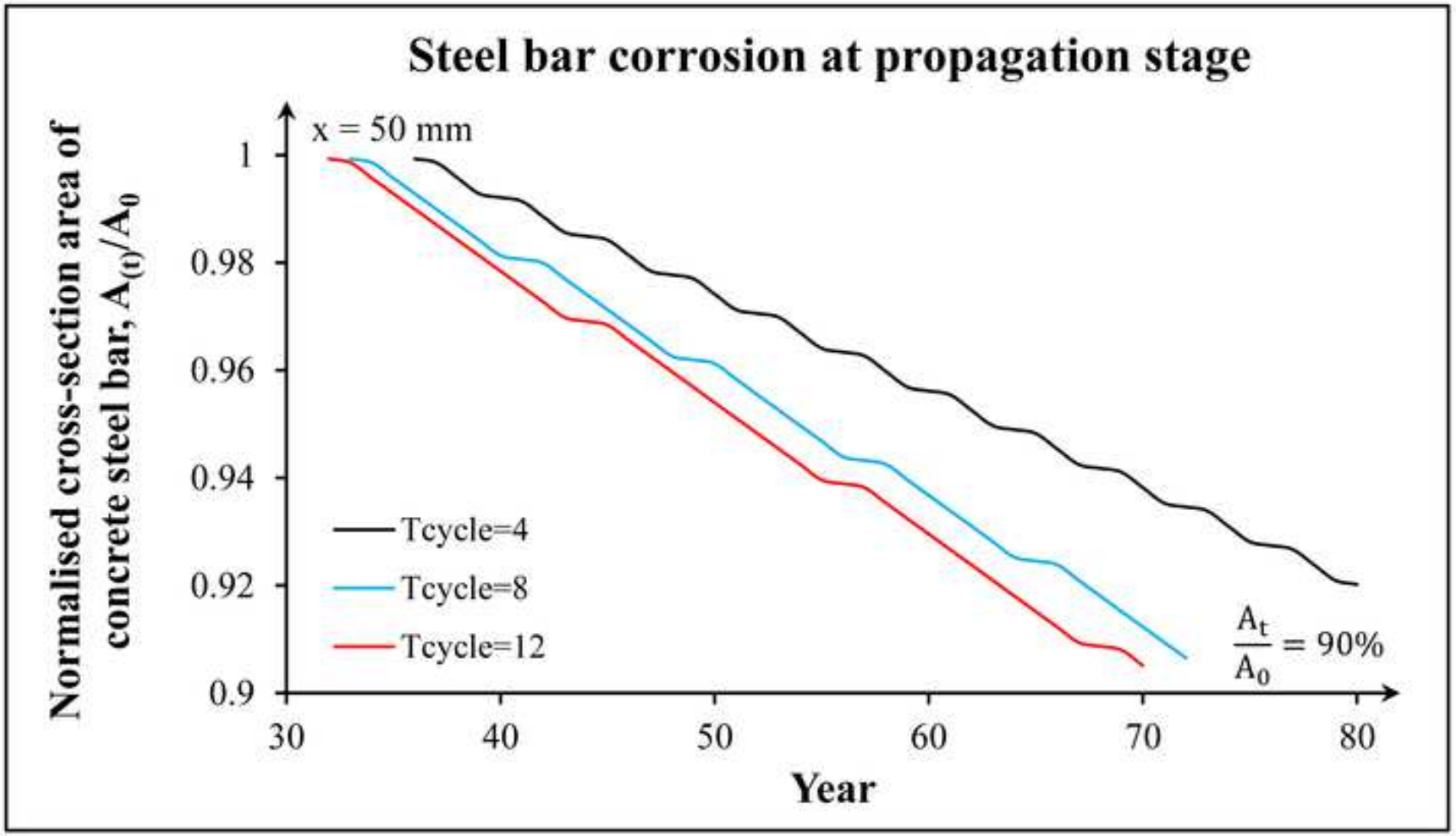

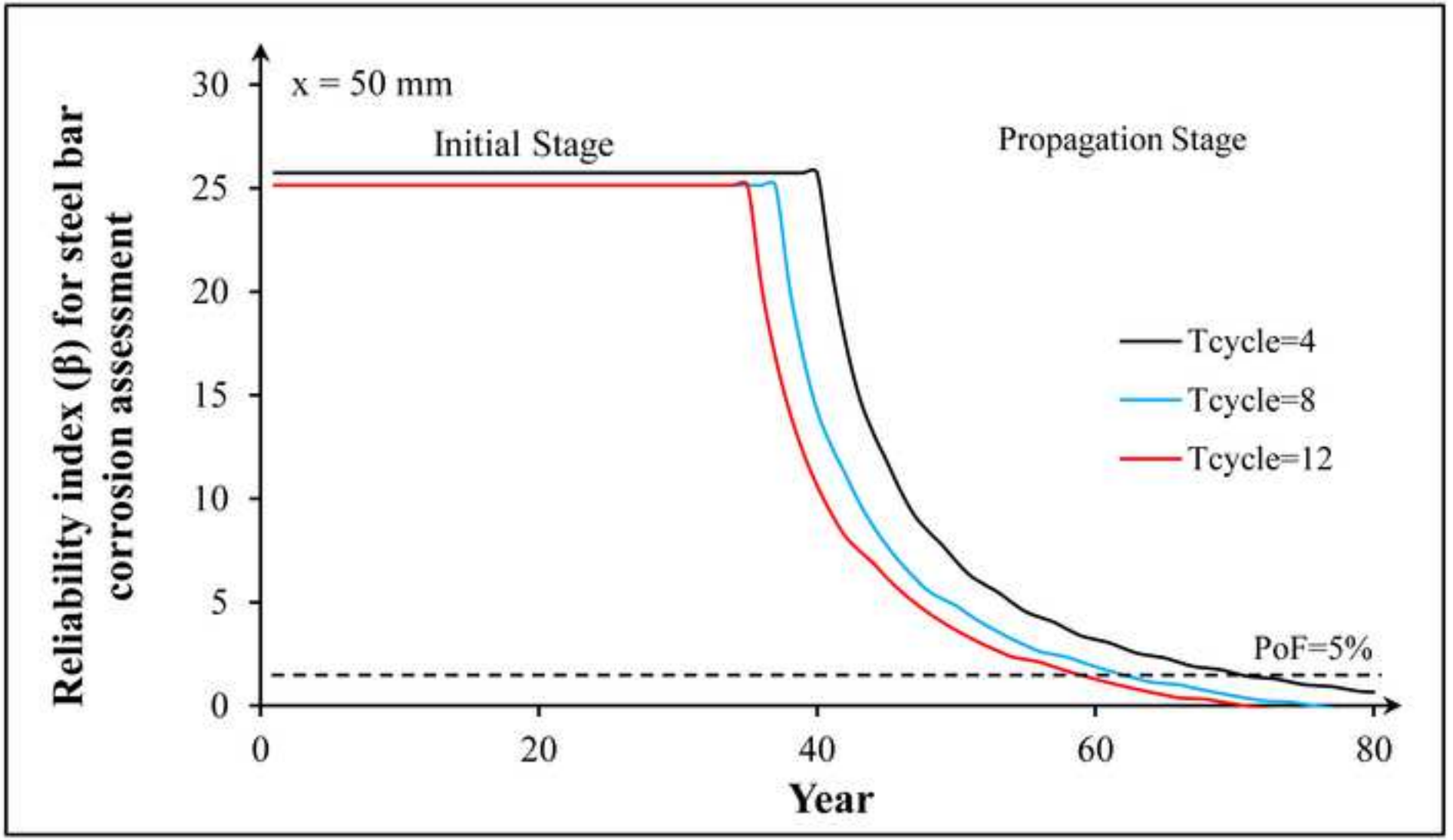

Figure

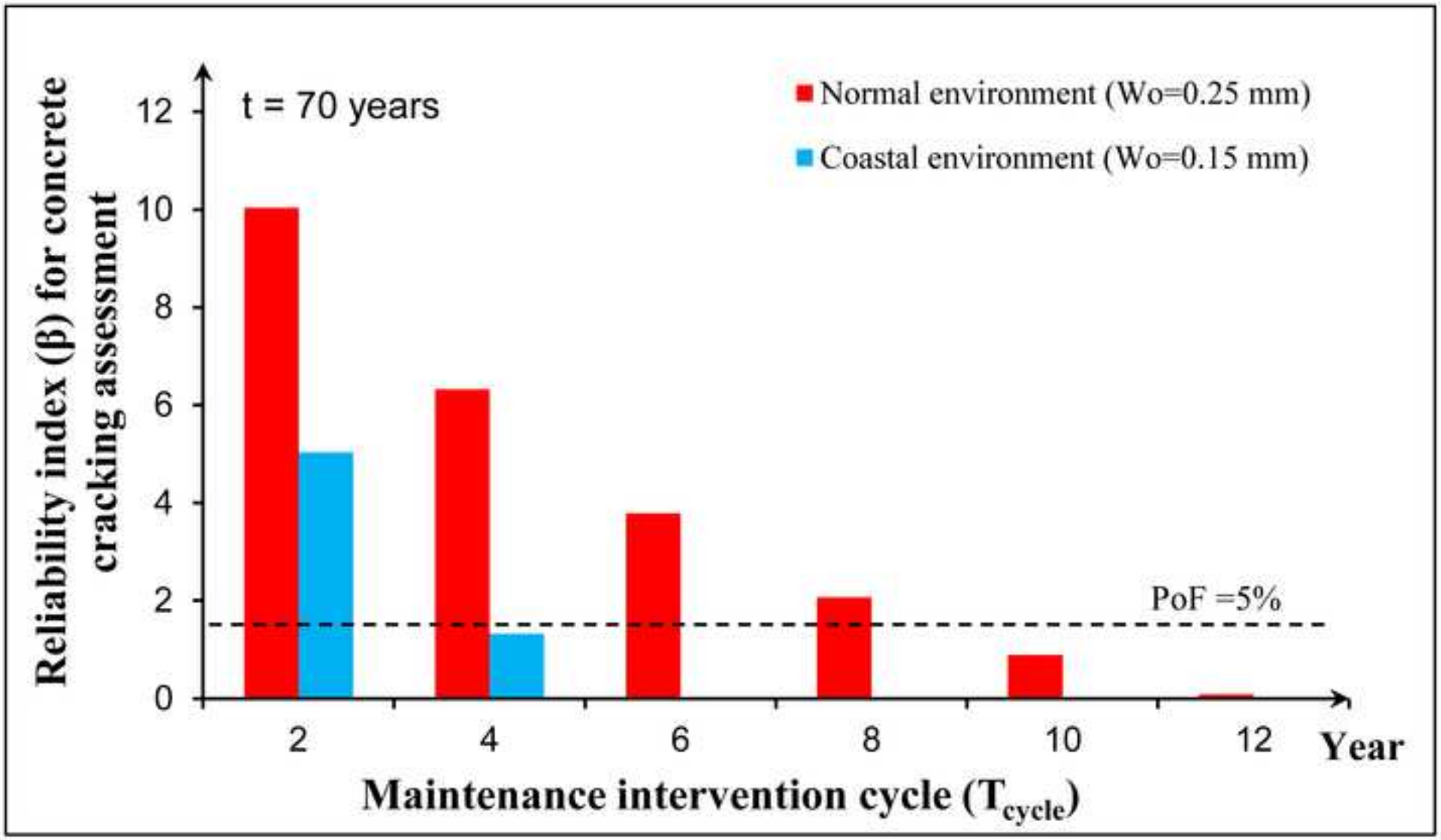

Figure